UNCLASSIFIED

Westinghouse

ELECTRIC CORPORATION

3845
FMD-18010
ARPA Order No. 80-59

Semiannual Report No. 2
on

PHOTOEMISSION SOLAR ENERGY CONVERTER

for the period

1 January 1960 through 30 June 1960
Project No. 3A99 09 001
Task No. 3A99 09 001 03
Contract No. DA-36-039-SC85248
8 September 1959-$86,183.00

15 July 1960

Special Electron Devices Section
Electronic Tube Division
Westinghouse Electric Corporation
Baltimore 3, Maryland

Power Sources Division
Electron Components Research Department
U.S. Army Signal Research and Development Laboratory
Fort Monmouth, New Jersey

The work performed under this contract was made possible by the support of the Advanced Research Projects Agency under Order No. 80-59, through the U.S. Army Signal Research and Development Laboratory.

TABLE OF CONTENTS

SECTION I. PURPOSE

SECTION II. ABSTRACT

SECTION III. PUBLICATIONS, LECTURES, REPORTS, AND CONFERENCES

SECTION IV. FACTUAL DATA

TABLE OF CONTENTS (Continued)

SECTION V. CONCLUSIONS

SECTION VI. PROGRAM FOR THE NEXT INTERVAL

SECTION VII. IDENTIFICATION OF PERSONNEL

APPENDIX A. EQUIVALENT CIRCUIT FOR PHOTOELECTRIC GENERATOR

APPENDIX B. AUTOMATIC READOUT VACUUM MONITORING SYSTEM

APPENDIX C. CLEANING AND HANDLING TECHNIQUES

LIST OF ILLUSTRATIONS

LIST OF ILLUSTRATIONS (Continued)

LIST OF TABLES

SECTION I

PURPOSE

In view of the considerable amount of solar energy flux in the vicinity of the earth's orbit, it would be desirable to have devices capable of converting this solar energy into electrical energy. This study is concerned with the feasibility of one such method of conversion employing the photoelectric effect and the construction of an experimental photogenerator using available material and techniques. This photogenerator is expected to have useful efficiency and a high power-per-unit-weight of generator, thereby being particularly suited for space application.

This study has been divided into three major tasks: Task A dealing with preliminary studies; Task B having as a goal, a sealed-off glass photogenerator with which the concept of photoemissive power generation can be tested; and Task C having as a goal a sealed-off plastic photogenerator. Each task is further subdivided into phases.

Phase 1 of Task A is concerned with an electron-optical study of the photogenerator in an effort to find the optimum electrode configuration.

Phase 2 of Task A bears upon the processing of the electrodes, and the deposition of the proper coatings upon them.

Phase 3 of Task A is the construction and use of a processing mechanism within the vacuum system, and the vacuum system itself.

Phase 1 of Task B will test the photoemissive generator concept, using demountable electrodes within a demountable vacuum system. Movement of the electrodes within the vacuum system will be accomplished by using the results of Phase 3, Task A.

Phase 2 of Task B will investigate a number of methods of extracting a sealed-off photogenerator from the vacuum system as well as different sealing methods.

In Task C, Phase 1 will be devoted to the study of the suitability of plastic for a vacuum envelope, and its compatability with photosurface materials.

The environment of space and its effect on both the vacuum envelope and the photosurface will be considered in this phase.

Phase 2 of Task C will pertain to the construction of a sealed-off plastic photogenerator.

SECTION II

ABSTRACT

The use of photoemission as a method of converting solar photon flux into electrical power and the development of a high power-per-unit-weight unit suitable for space use are considered in this study. Experimental results using the WX-3964 photogenerator are presented, showing that one tube, having a relatively wide spacing of 70 mils, supplied output power of over 125 microwatts at an efficiency of 0.01 percent. A description of an experiment in the bell-jar processing station is presented herein, and the operation of the automatic readout experiment is described. Steps leading to the manufacture and processing of the anode and photocathode are described, as well as the construction of the WX-4209, a thin glass-sandwich photogenerator. Changes in processes and procedures are noted, and work leading to an equivalent circuit for the photogenerator is given.

SECTION III

PUBLICATIONS, LECTURES, REPORTS, AND CONFERENCES

On 4 January, a meeting was held between Westinghouse and Signal Corps representatives at Fort Monmouth to discuss the format of the semi-annual report. Present from Westinghouse were Messrs. C. Arthur and I. Limansky. Representing the Signal Corps Power Sources Division were Dr. Emil Kittl and Mr. Stuart Shapiro.

On 11 April, Dr. Emil Kittl and Stuart Shapiro visited the Special Electron Devices section to discuss and observe photogenerator project progress.

On 9 and 10 May, I. Limansky visited the Camera Tube Section, Elmira, New York, to discuss results obtained with the WX-3964 photogenerators with Messrs. J. Hall and H. Shabanowitz.

On 17 to 19 May, Dr. A. S. Jensen, I. Limansky, and E. Wood attended the Fourteenth Annual Power Sources Conference given at the Shelburne Hotel, Atlantic City, New Jersey. On 17 May, "Photoelectric Conversion," a paper by Dr. A. S. Jensen and I. Limansky was presented at the Solar Energy Conversion Session.

SECTION IV

FACTUAL DATA

4.1 INTRODUCTION

The close spacing required in the photogenerator imposes stringent limitations with regard to the manner of processing this tube. If it is to be a few mils thick in its final form, as the theoretical study indicates, a host of problems arise as to the sealing method, photosurface formation, etc. Even when the tube vacuum envelope is relatively thick, many of the same problems are encountered. This report describes the design of the tube under investigation, the problems encountered in its processing and construction, and how these problems were resolved.

It will be seen that this investigation is composed of three parallel investigations, (1) photogenerators WX-3964 constructed in an image orthicon front end, (2) experiments in the bell-jar, and (3) photogenerators WX-4209 made in the form of a thin glass sandwich. The first investigation is intended to determine the surface conditions of the electrodes necessary for photogenerator operation and can be utilized to test the photogenerator concept. The second investigation tests the photogenerator concept directly, since the anode and photocathode processed within the bell-jar can be positioned relative to one another by means of manipulators extending into the bell-jar. It is therefore possible to determine the effect of spacing upon the output power of the photogenerator.

The third investigation is concerned with the construction and processing of a thin glass-sandwich photogenerator that may be removed from the bell-jar processing station where it is assembled and sealed. The first designs are to be made of thick glass, while subsequent designs will use thin glass.

For purposes of this report, information is reported according to task-phase as noted in Section I. The first investigation is a part of Task A, Phases 1 and 2, since the WX-3964 can be considered as an electron-optical study as well as dealing with the processing of electrodes. The second investigation is contained within Task B, Phase 1, while the third investigation is encompassed by Task B, Phase 2 and Task C.

4.2 TASK A - PRELIMINARY STUDIES

4.2.1 Phase 1 - Electron Optics

Work with the rubber-membrane potential model has been temporarily deferred until more information is available regarding the effect of the surface conditions on the anode. Sufficient qualitative experiments were run to ascertain that the electrons will strike the rear surface of the anode if a negative charge of some description exists behind the anode. However, in order to insulate the anode from the photocathode, it is necessary to apply an insulating coating on the side of the anode facing the photocathode to maintain the small spacing between the two. The characteristics of this coating and its action within the tube are not known with any exactness. It may be that the silicon monoxide coating with a layer of cesium might emit photo-electrons, thus charging itself positively, or, conversely, it might be charged negatively by the incidence of photoelectrons released by the photocathode. Preparations are being made to determine the role played by the insulating coating upon the anode.

Two alternate electron optical models exist, and both require the making of a photogenerator. One model is the WX-3964 that is described in a later section, while the other model is the demountable tube processed in the bell-jar station. Until data is forthcoming from these models, no firm basis can exist for the assignment of the potentials within the tube, and no meaningful results can be obtained from the rubber-membrane potential model.

4.2.2 Phase 2 - Electrode Processing

Prior to the assembly of the photogenerator, the electrode surfaces must be prepared in a certain manner to ensure the proper characteristics. The tentative processes and techniques were described in the first semiannual report, results will be reported here, and the revisions may be found in Appendix C.

4. 2. 2. 1 Photocathode

The photocathode has been chosen to be manganese-antimony-cesium evaporated upon a glass substrate upon which a 10 mesh-per-inch copper mesh has been applied beforehand. It was thought that it would be necessary to add a transparent conducting coating to the glass substrate and mesh; i. e., tin oxide, but this is not being done in the first experiments, since it is believed that the addition of manganese performs the same function. It may be necessary to add a thin film of gold, however, to block the infrared photons and thereby reduce the space charge caused by low-velocity electrons emitted from the photocathode. Again, this will not be done unless deemed necessary from the experimental results.

Several glass substrates were processed as follows: first, nichrome or chromium were deposited in vacuum upon a glass disc to approximately 95-percent transmission, then copper was evaporated over the thin film. The chromium was necessary to provide good adhesion of the copper to glass. The glass disc was then coated with Kodak photoresist, and exposed to ultraviolet light through a negative having the 10 mesh-per-inch pattern on it. The photoresist was then washed off using trichlorethylene, and the glass disc was etched using ferric chloride 4° Beumé, diluted 4 to 1 by volume with water. The remainder of the photoresist was then removed using trichlorethylene and brushing with a camel's-hair brush. Figure 1 shows a completed glass substrate with mesh.

Adhesion was the problem with this method; sufficient chromium evaporated upon the glass substrate would provide a tenacious copper film-glass bond, but would also cut down the light transmission. Evaporation of the chromium was performed using a tungsten basket which did not permit good heat transfer to the chromium. This, in turn, caused the surrounding components to outgas locally, since they were heated by radiation from the evaporator. Work is underway to place chromium upon a

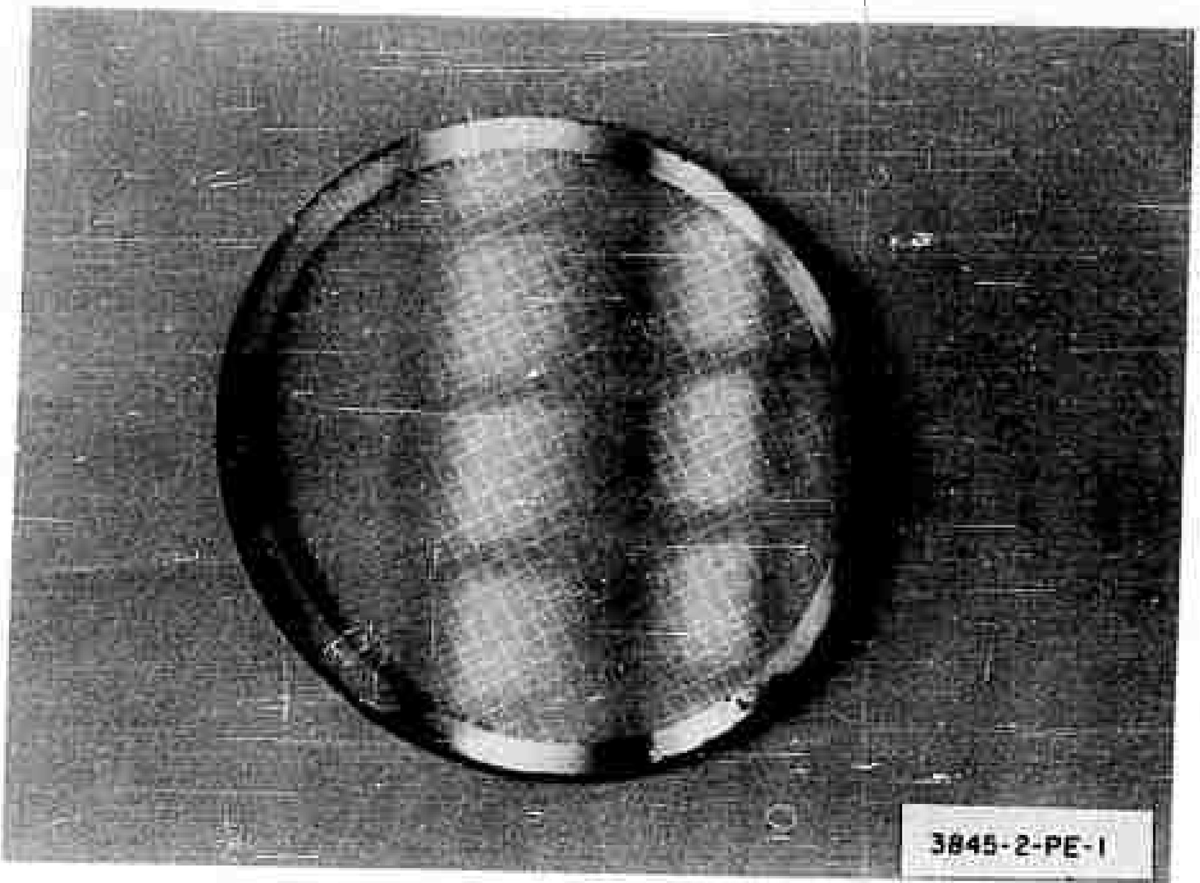

Figure 1. Photocathode Substrate With Mesh

thin tungsten wire, the combination to be used for the chromium evaporator.

During the bell-jar experiment to be described later, manganese and antimony were evaporated on one of the glass substrates described above and the light transmission monitored using a light-transmission measuring setup shown in figure 2. The light source was powered from a constant voltage source, and the output of the photoconductive cell was fed into the Weston Recorder that is part of the automatic readout system. A projection lens focused the light reflected by the mirror onto the Clairex cell and materially aided to reduce the effect of ambient light upon the readings. The glass substrate could be moved inside the bell-jar so that the overall transmission could be measured before and after evaporation. This was found useful, since the photoconductive cell exhibited fatigue upon

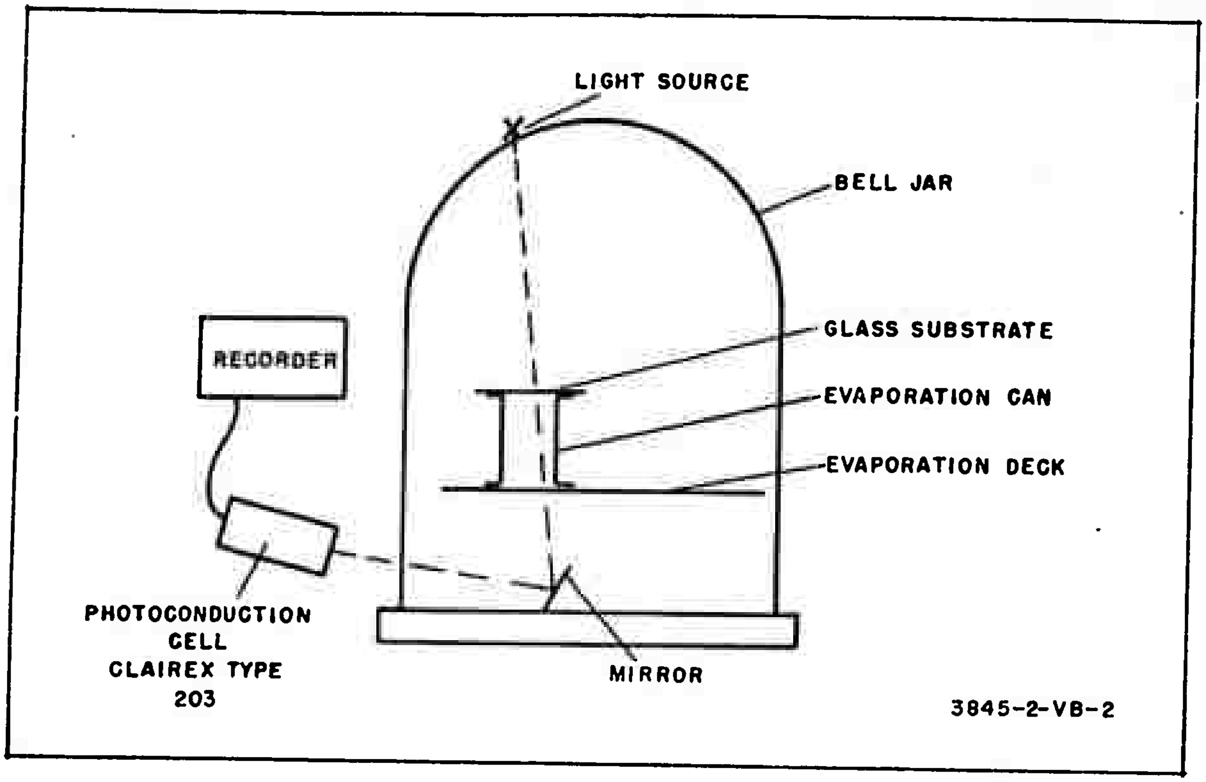

Figure 2. Light-Transmission Measuring Setup

being exposed to light, the fatigue showing up as a slow change in output reading with time. It was possible to compensate for this fatigue by using the chart recorder and checking the total transmission after evaporation by displacing the glass substrate.

4.2.2.2 Anode

Due to the close spacing between anode and photocathode and the necessity of keeping the low work-function material away from the incident light, the anode should be made of a wire mesh with an insulating coating on the side facing the photocathode, and the low work-function material should be on the side away from the photocathode. Silver-oxygen-cesium was chosen as the active material for its low quantum efficiency and work function, and silicon monoxide for the insulating coating. The mesh for the WX-4209 is woven stainless steel, 100 mesh per inch; the mesh for the WX-3964 is copper, 400 mesh per inch.

The silver can be applied to the anode mesh either as a vacuum-evaporated coating or by electrolytic plating. Figure 3 is a photograph of the WX-4209 anode mesh having a silver-plated anode and a silicon monoxide coating upon the face closest to the photocathode.

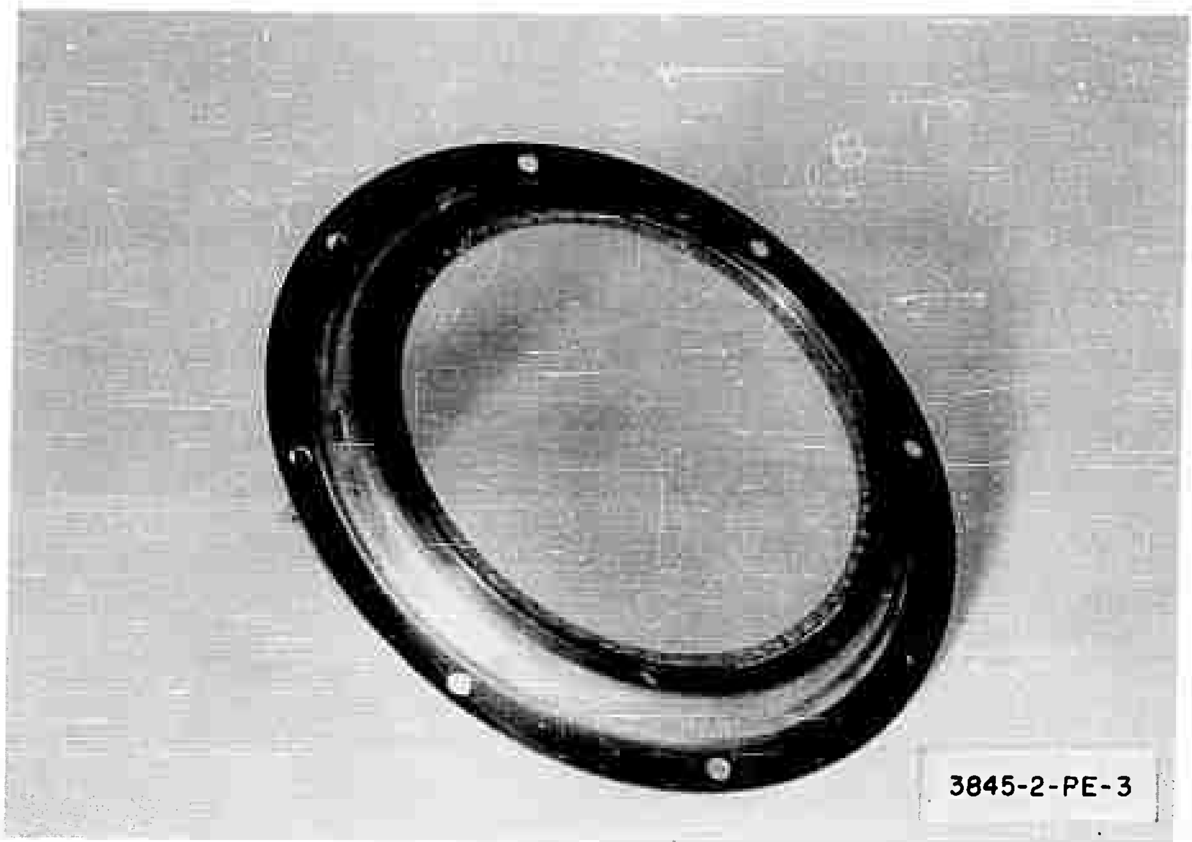

Figure 3. Anode Mesh Welded to Anode Mesh Support, WX-4209

4.2.2.3 WX-4220 Photoemission Control Tube

This tube is intended to act as a check on the photocathode processing during the course of this program. Photocathodes are to be formed inside the WX-4220 and tested for photoelectric emission - expressed in microamperes per lumen. This procedure will enable us to determine the quality of our photocathodes with respect to the rest of the industry and to note any changes with changes in processing.

The tentative specifications and drawings of this tube were given in the first semiannual report. Figure 4 is a photograph of a completed tube. Some difficulty was experienced in the choice of evaporators to be included, since the current necessary to evaporate the metals must not exceed the stem lead current-carrying capacity. This ruled out the use of the tungsten conical baskets normally used in the bell-jar station for manganese evaporation. In their place, 20-mil tantalum wires have been plated with manganese.

As yet, no WX-4220 tubes have been completely processed due to the emphasis placed on the bell-jar experiment to be described in a later section.

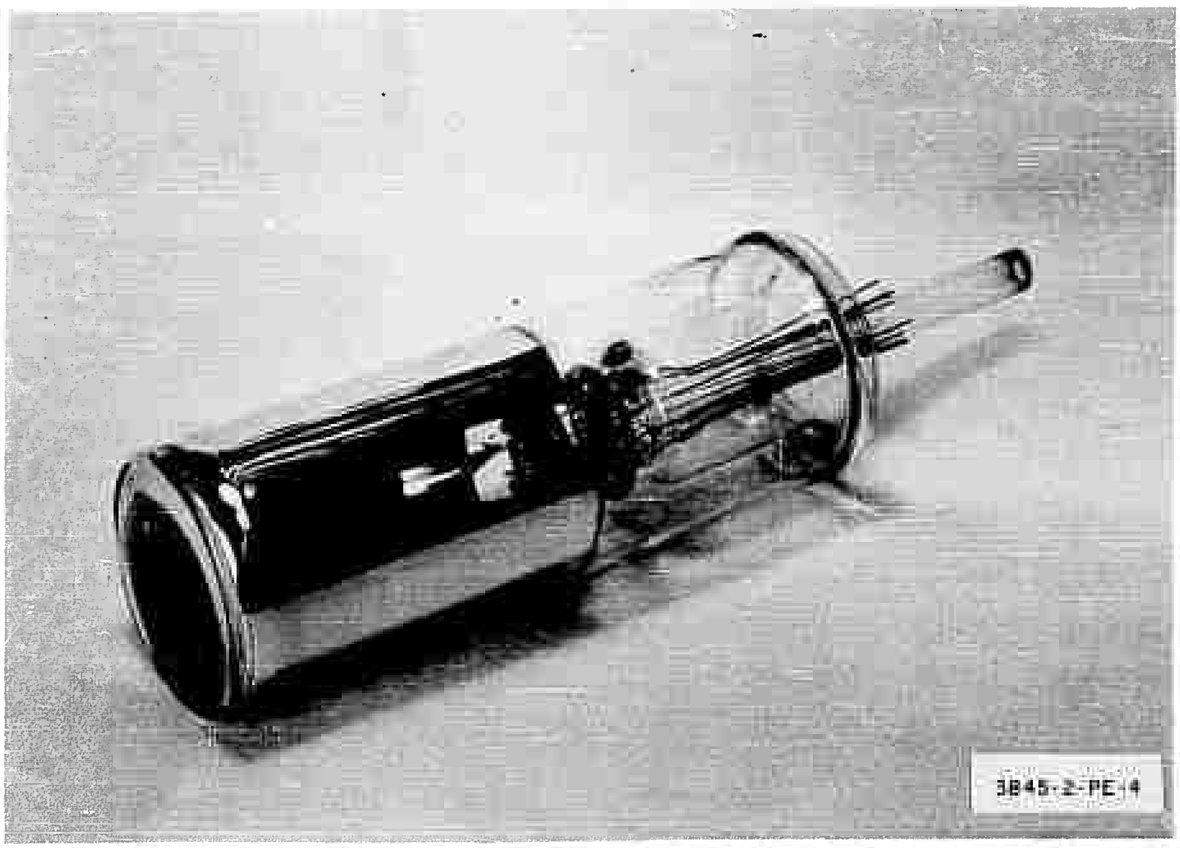

Figure 4. Photoemission Control Tube, WX-4220

4.2.2.4 Experimental Results - WX-3964

The WX-3964 was originally intended to determine the effect of the anode surface upon photogenerator action. Six tubes were made by the Camera Tube Section: two having the insulating coating on the anode facing the photocathode; two having the insulating coating facing away from the photocathode; and two having no insulating coating at all upon the anode. Unfortunately, variation in the results precluded any firm decision as to the proper anode surfacing; however, several points of interest were noted and new experimental and theoretical techniques devised to describe the operation of the photogenerator.

Table 1 gives the results obtained with the six WX-3964 photogenerators using the sun as a light source. Figures 5 through 9 present the curves of power versus load resistance and apparent internal resistance versus load current for all tubes except No. 6 which was inoperable. Figure 10 depicts schematically the measuring setup that was used. For comparison, figure 11 shows the results of measurements made using the Westinghouse sunlamp.

Preliminary electrical measurements (figure 11) made on the WX-3964 made in February gave no useful information as to the effect of anode surfacing upon photogenerator action, particularly since tubes No. 1 and 6 gave little and no output, respectively. In an effort to find the cause of the variation, the simplest equivalent circuit was assumed for the photogenerator - that of a voltage generator in series with a resistance, r_{int}, the value of which would depend upon the current flowing through it (see figure 10). The open circuit voltage E would depend upon the highest frequency of light reaching the photocathode, and the value of A would depend upon the spacing, and the quantum efficiency of the photocathode. Also, the square root term was not assumed in the beginning, but a log-log plot of apparent internal resistance

$$r_{int} = \frac{V_{oc} - V}{I_L} \qquad (4\text{-}1)$$

TABLE 1

RESULTS OBTAINED WITH THE SIX WX-3964 PHOTOGENERATORS

TUBE	ANODE CONDITION	PHOTO-RESPONSE AT 130V (μA/l)	MAX POWER OUTPUT (μW)	LOAD RES. AT MATCH (KΩ)	IRIS FOR MAX POWER	SPACING (mils)	AREA (cm^2)
4	No insulation	10	130	1.0	Open	69	21.2
5	No insulation	39	4.4	16	3	73	23.8
1	Insulation facing photocathode	13	2.2	70	3	108	23.8
6	Insulation facing photocathode	13	0	-	-	92	24.6
2	Insulation opposite photocathode	2.8	40	1.6	1	89	20.5
3	Insulation opposite photocathode	2.6	29	1.5	Open	109	20.5

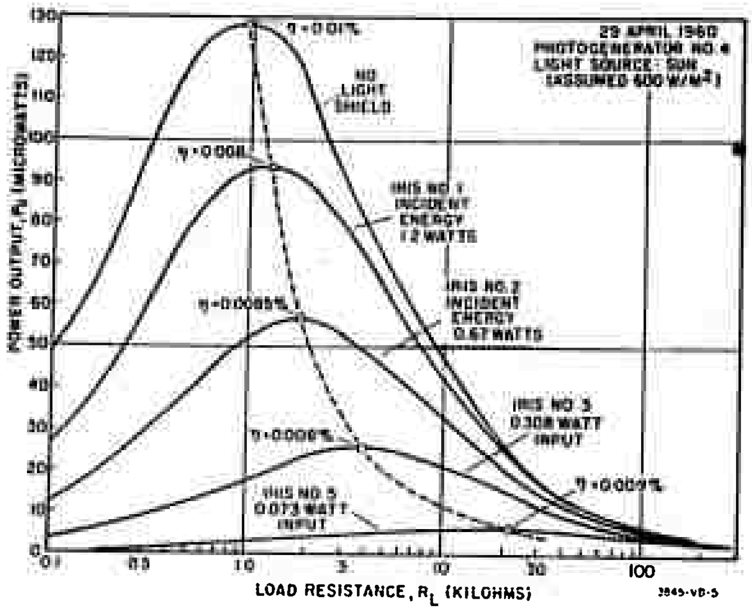

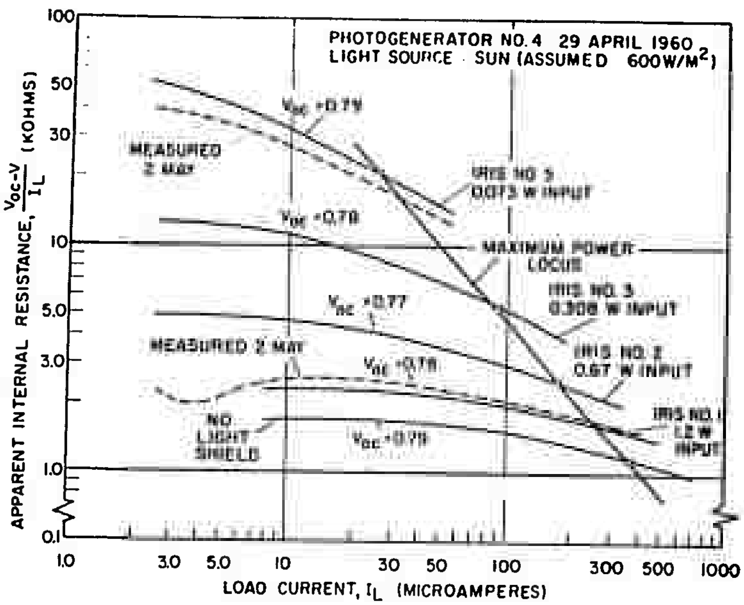

Figure 5. Experimental Results, WX-3964, No. 4, (a) Power Output vs Load Resistance, (b) Apparent Internal Resistance vs Load Current

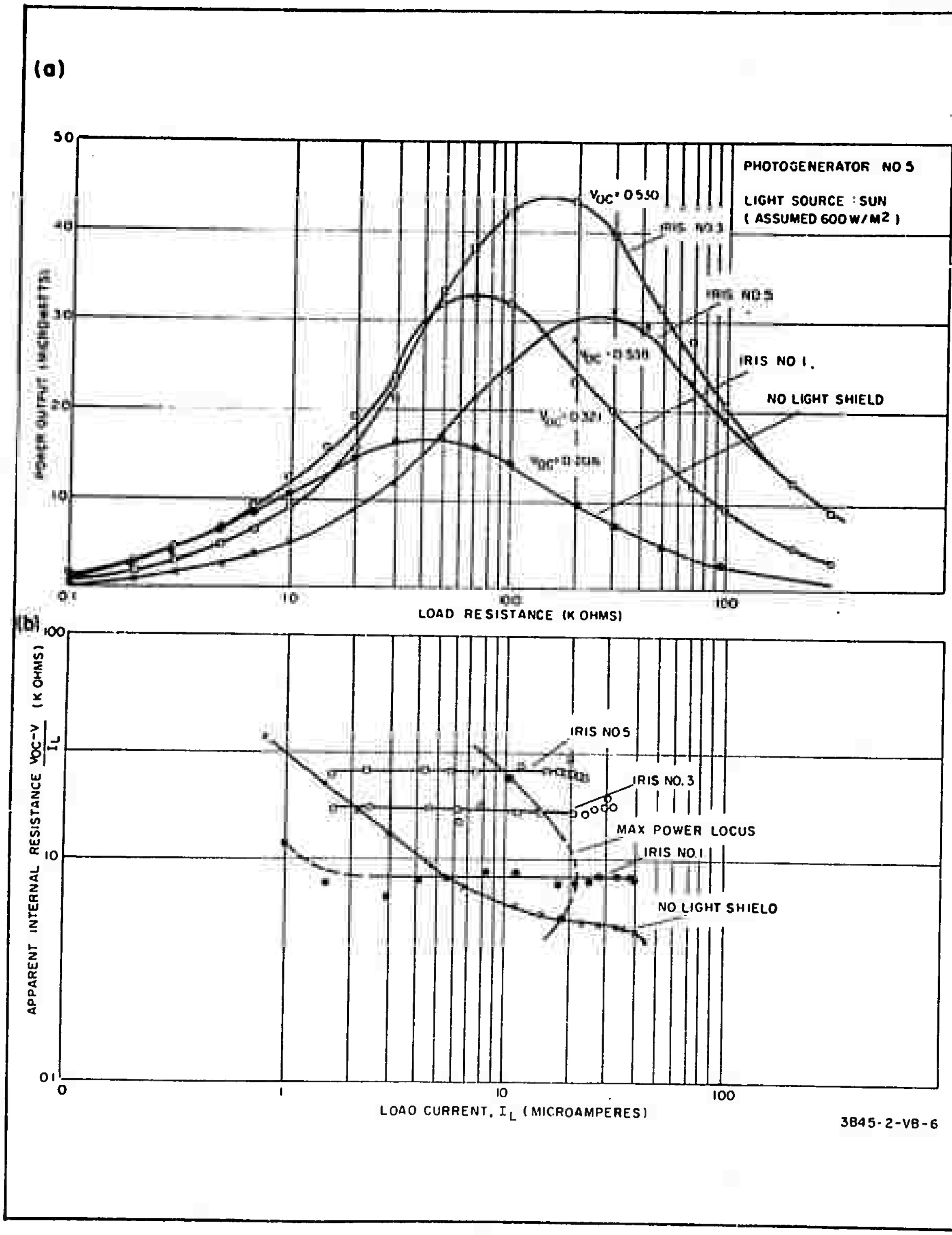

Figure 6. Experimental Results, WX-3964, No. 5, (a) Power Output vs Load Resistance, (b) Apparent Internal Resistance vs Load Current

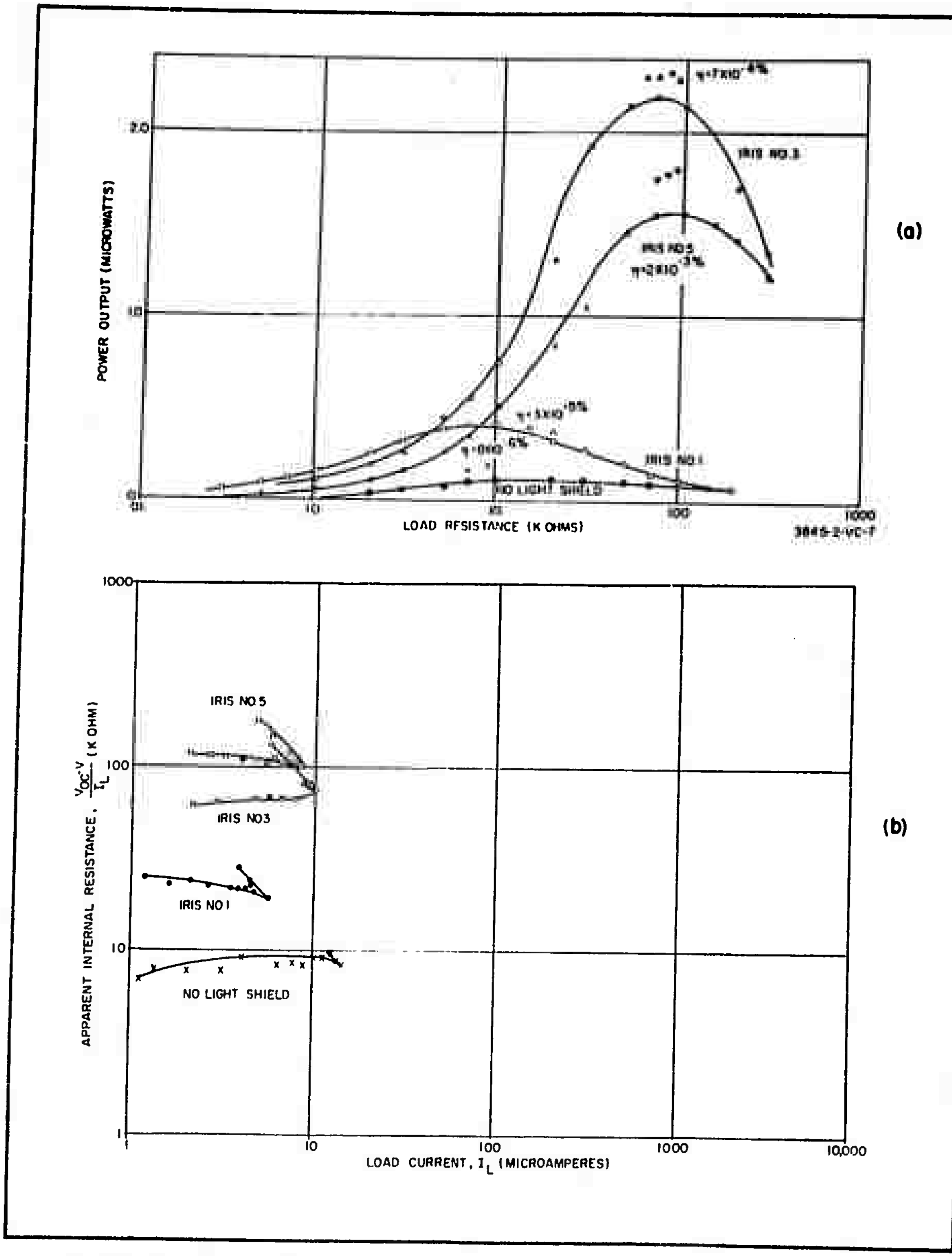

Figure 7. Experimental Results, WX-3964, No. 1, (a) Power Output vs Load Resistance, (b) Apparent Internal Resistance vs Load Current

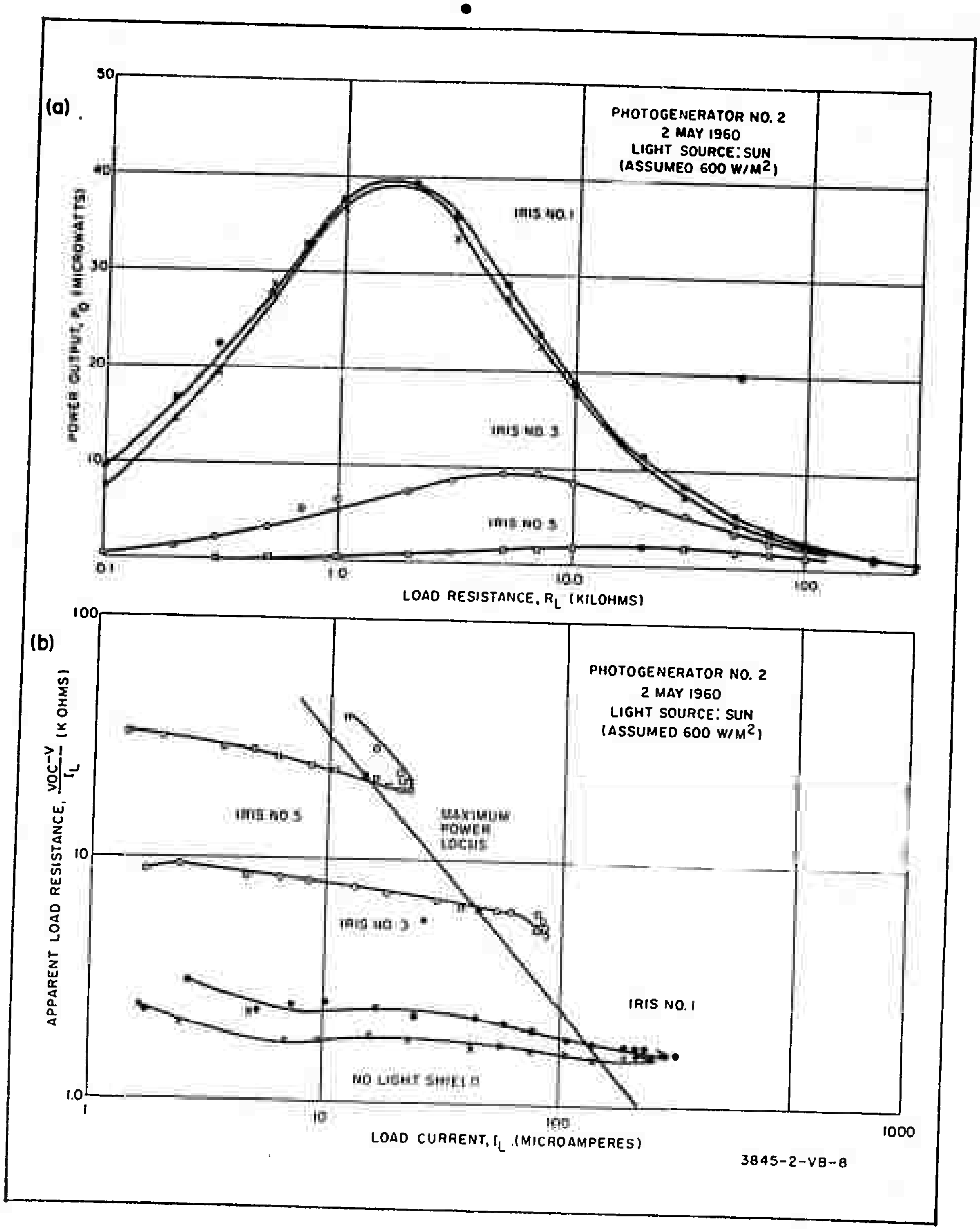

Figure 8. Experimental Results, WX-3964, No. 2, (a) Power Output vs Load Resistance, (b) Apparent Internal Resistance vs Load Current

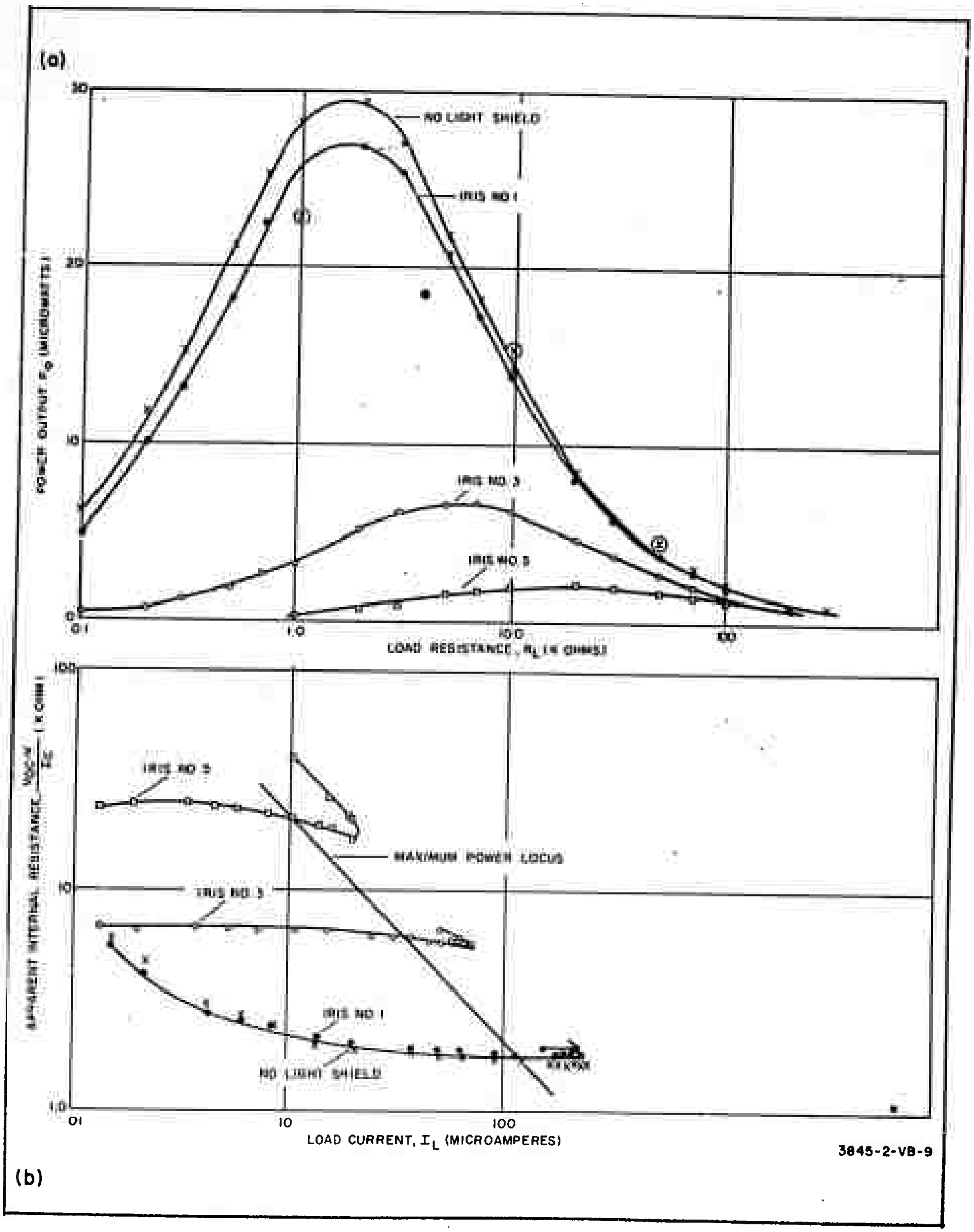

Figure 9. Experimental Results, WX-3964, No. 3, (a) Power Output vs Load Resistance, (b) Apparent Internal Resistance vs Load Current

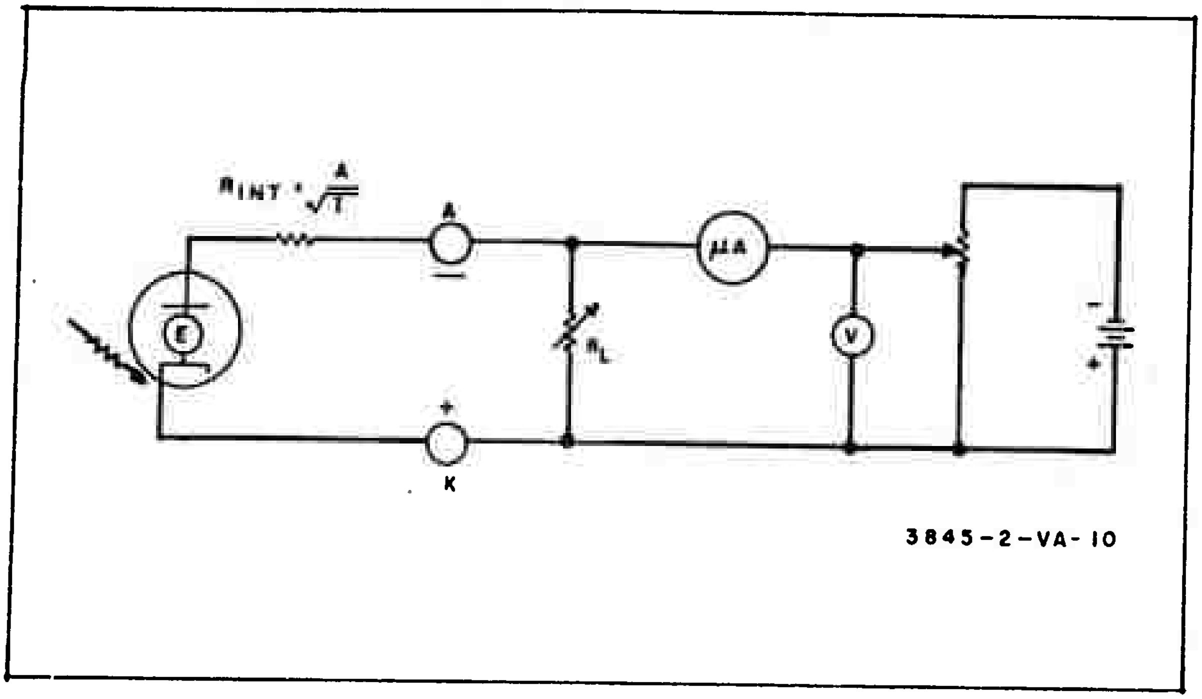

Figure 10. Schematic of Photogenerator Electrical Measuring Setup

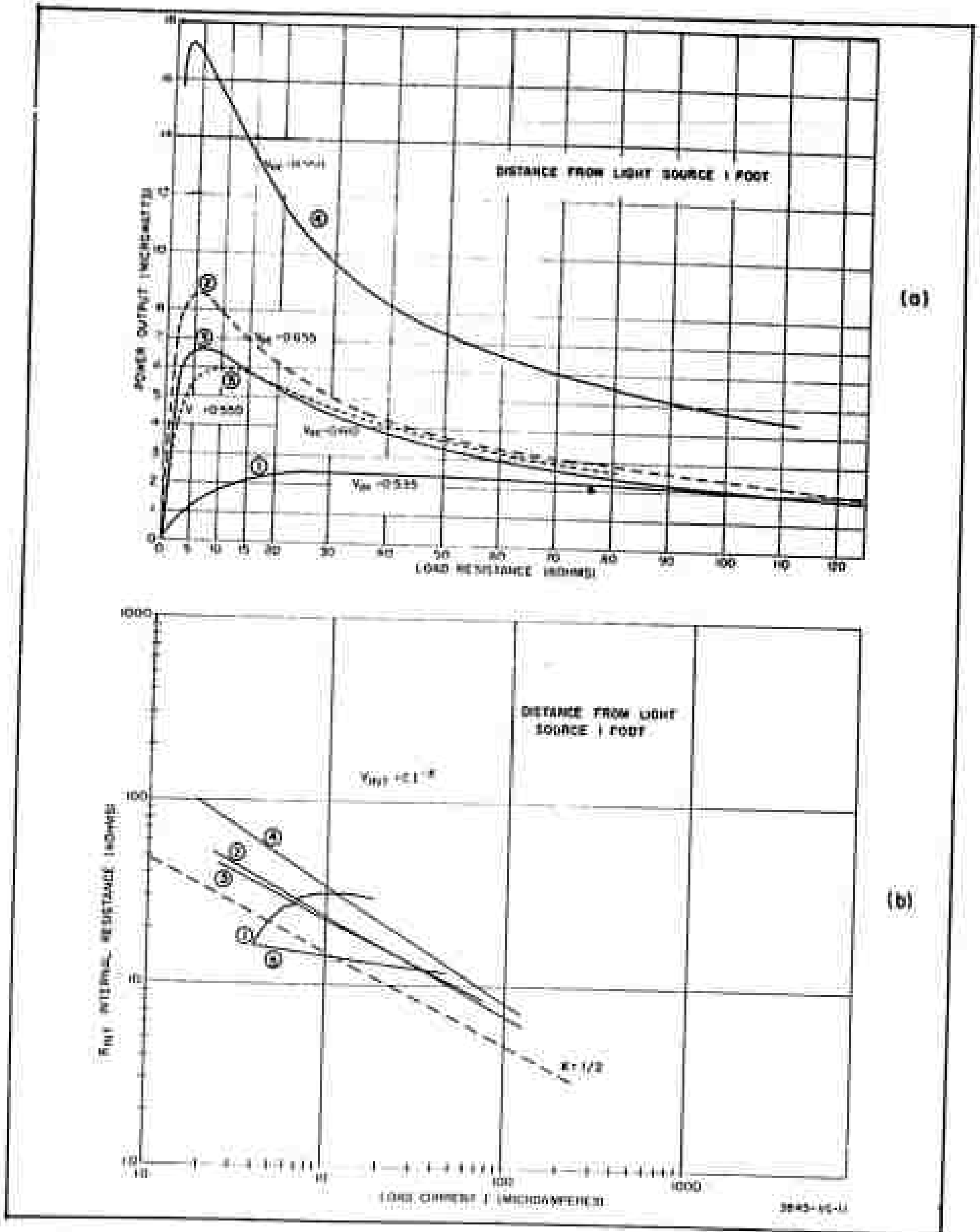

Figure 11. Early Experimental Results Using Westinghouse Sunlamp, (a) Power Output vs Load Resistance (b) Apparent Internal Resistance vs Load Current

versus load current was made as shown in figure 11b. It may be seen that the plots for tubes Nos. 2, 3, and 4 approximately follow the equation

$$r_{int} = \frac{A}{I_L^{1/2}} \tag{4-2}$$

but that tubes Nos. 1 and 5 deviate strongly. In fact, repeated measurements of tube No. 1 showed that a change was taking place; at low currents, the internal resistance as computed by equation 4-1 was lower than that predicted by equation 4-2. In addition, it was found that uncollimated light (produced by moving the light source closer to the tube) caused a decrease in open-circuit voltage. It is suspected that the uncollimated light struck the internal structure (used in the WX-3964 as supports for the anode screen and evaporators and not necessary to the final design of the photogenerator) which then emitted photoelectrons that produced a reverse current, thus reducing the net power output. Analysis of the circuit containing reverse current (Appendix A) showed that this mechanism would be capable of explaining the change in open-circuit voltage and the decrease in internal resistance of the tube at low currents.

Although potentially useful, the equivalent circuit approach did not explain the experimental variability directly. Only comparison of tubes 2, 3, and 4 with tubes 1 and 5 on the log-log plot of internal resistance versus load current showed that the internal resistance was essentially constant with load current for tubes 1 and 5, indicating the presence of a large series resistance tending to swamp the normal variation of internal resistance of the tube. Indeed, this was found to be the case, since tubes 1, 5, and 6 have a larger aperture in the contact ring than the other three tubes, so it is probable that the photocathode surface could not make good contact. This may be seen in figure 12, a photograph of photogenerator No. 6 after autopsy; the evaporated photocathode may be seen as a concentric shaded area within the contact ring aperture, with a clear area

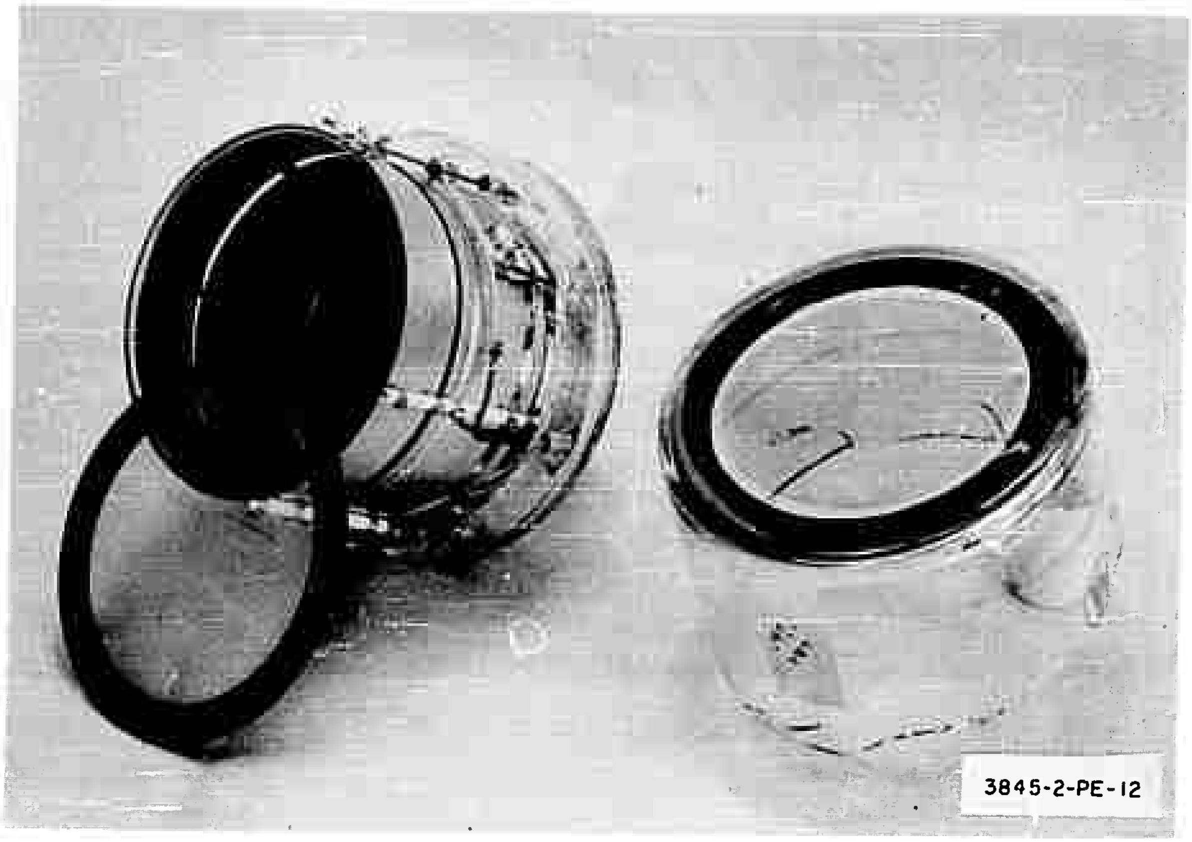

Figure 12. Autopsied WX-3964 Photogenerator, No. 6

between the two, indicating little if any photosurface deposited there. Tube No. 6 showed no photogenerator action.

It may be inferred that the geometry of the tube (i. e., the mesh anode being so close to the photosurface) did not permit good photosurface contact. This was corrected by the Camera Tube Section in tubes 2, 3, and 4 by decreasing the size of the aperture. The presence of the mesh between the photocathode substrate and the evaporators also appears to have decreased the photoemission, as may be seen by reference to table 1.

Table 1 also has a column giving the distances between the anode mesh and photosurface for the tubes. There appears to be a definite relationship between power output and spacing, although it is too risky to assign any values on the basis of the three tubes (Nos. 2, 3, and 8). Nine more WX-3964 photogenerators having movable anode meshes and a smaller aperture in the contact ring have been ordered from the Camera Tube Section. The tubes have been designed so that the distance between anode and photocathode can be made larger during processing, thereby improving the evaporation geometry. During electrical measurement, the spacing can be made smaller for more efficient photogenerator action.

It may be seen therefore that although the WX-3964 has not given any usable information regarding the anode surface conditions, it has given valuable experience in the operation of the photogenerator and techniques of measurement. For example, the best WX-3964 photogenerator had an efficiency of 0.01 percent computed by assuming the sun's energy incident upon the tube as 600 w/m^2. Using a Westinghouse sunlamp at 1 foot, the incident energy is 800 w/m^2. (See figure 13.) The output of the photogenerator when illuminated by the sunlamp is fully an order of magnitude below the value of the output when the photogenerator is illuminated by the sun. This shows the necessity of using a sun-equivalent laboratory light source (if available) when making measurements for the purpose of computing the efficiency of the photogenerator. It should also be noted that the open circuit voltage of the photogenerator differed in the two cases, being larger for the sunlamp due to the higher amount of ultraviolet light emitted. Even if the sun is used as a light source, the value of the incident radiation upon the photogenerator should be measured with a pyrheliometer. This was not done for the above measurements, since the efficiency, being two orders of magnitude below the value that is ultimately expected, was too small to require extreme accuracy.

4.2.3 Phase 3 - Bell-Jar Processing System

Our experience with the WX-3964 photogenerator has shown us that forming a photocathode through a mesh gives poor results. This was anticipated at the beginning of this investigation, and provisions were made to have a vacuum system for processing which would permit the displacement of the photocathode away from the mesh during photocathode formation. At

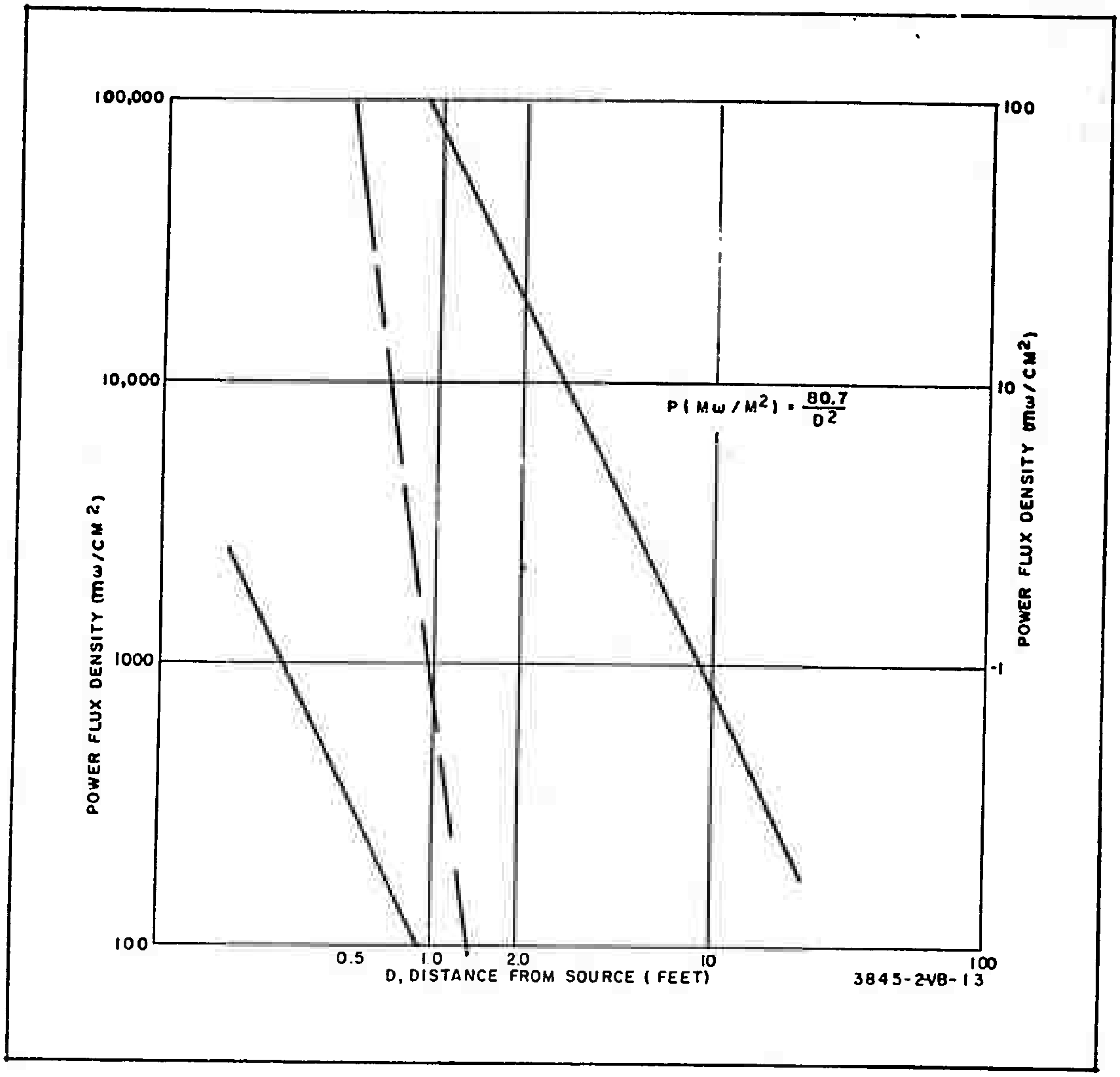

Figure 13. Calibration of Power Flux Density vs Distance, Westinghouse Sunlamp

the same time, this vacuum system should be capable of performing the various other preliminary evaporations necessary in the course of this program.

4.2.3.1 Mechanical Arrangement

The general configuration of the vacuum station was described in Semiannual Report No. 1 and has not changed materially. It consists of the vacuum station proper, the automatic readout system, and the electrical interconnections. The physical arrangement is shown in figure 14, and a sketch of the portion within the bell-jar is shown in figure 15. Although all stations have been used at one time or another, evaporation station No. 1 is habitually used for mangenese and antimony evaporation, while evaporation station No. 4 is used for the cesium evaporation during the bell-jar experiment. A special transport mechanism was designed but was not constructed due to a change in design of the WX-4209. This mechanism would have been capable of picking up and releasing the glass discs used as photocathode substrates and moving them over the appropriate evaporation stations. In its place, a very simple sheet metal (stainless steel) substitute was made that was entirely adequate for the purpose and used the minimum of material.

In spite of the large amount of material within the bell-jar, the vacuum system has been consistently reaching pressures in the order of 1 to 5 x 10^{-6} mm Hg with the aid of both a liquid nitrogen cold trap and a Zeolite trap, without having to bake out the bell-jar. This has been measured with an ion gauge contained within the bell-jar and checked against the manifold ion gauge reading.

4.2.3.2 Electrical System

The automatic readout system described in Semi-annual Report No. 1 has been operating satisfactorily and has permitted the most efficient use of the vacuum station. In figure 14, the automatic readout system is contained in the three chassis at the top of the rack. The top chassis contains the power supply, the middle chassis is the Weston strip chart recorder, while the third chassis contains the control and switching circuits. Appendix B gives the schematic diagram of this system, and figure 16 is an example of the strip chart record made by the unit during automatic operation. It is particularly useful in recording the progress of an important section of an experiment, for example, the light transmission through the glass substrate, during operation, while attention is directed to observing the process visually. Safety features are included that prevent turning on

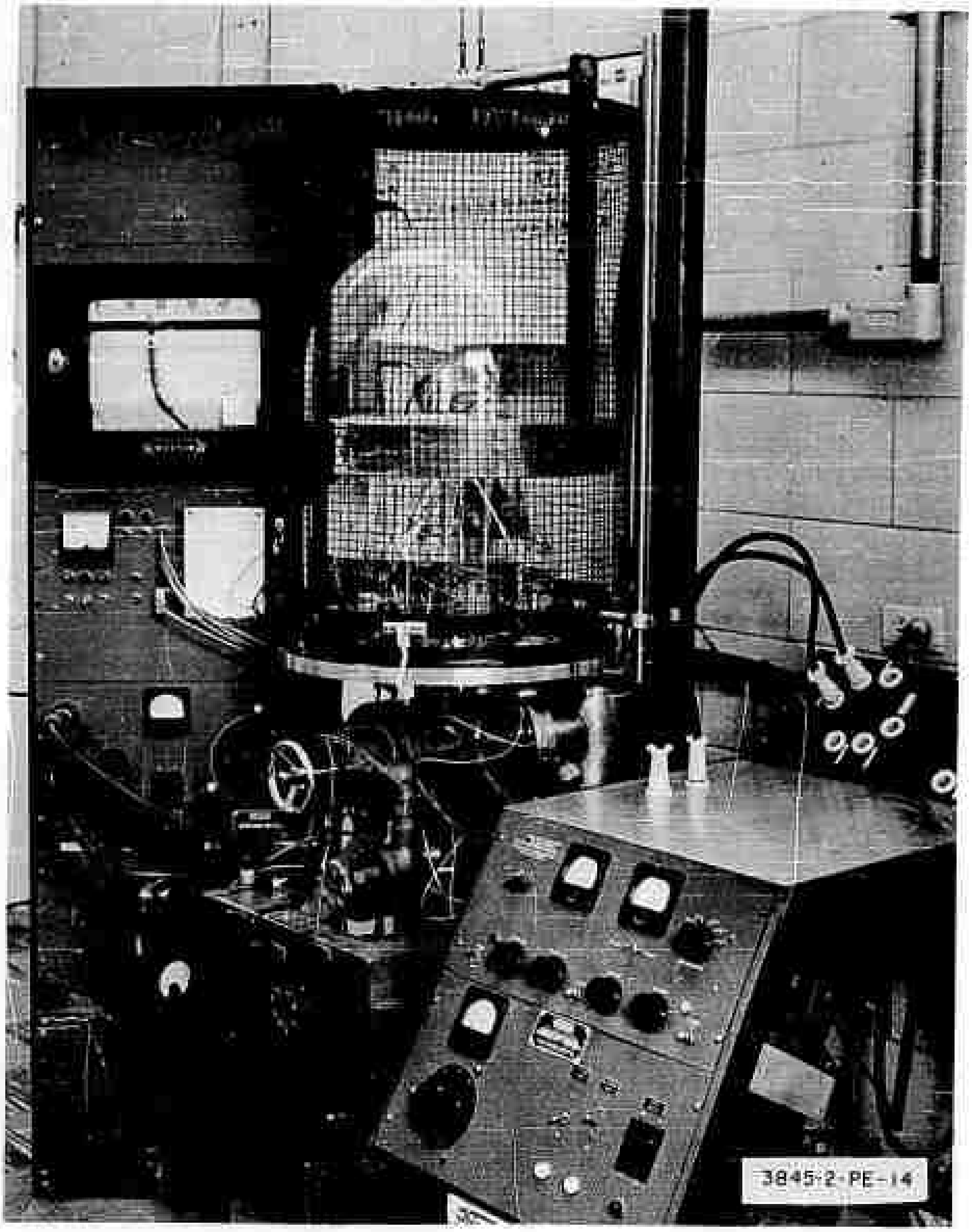

Figure 14. Bell-Jar Processing System

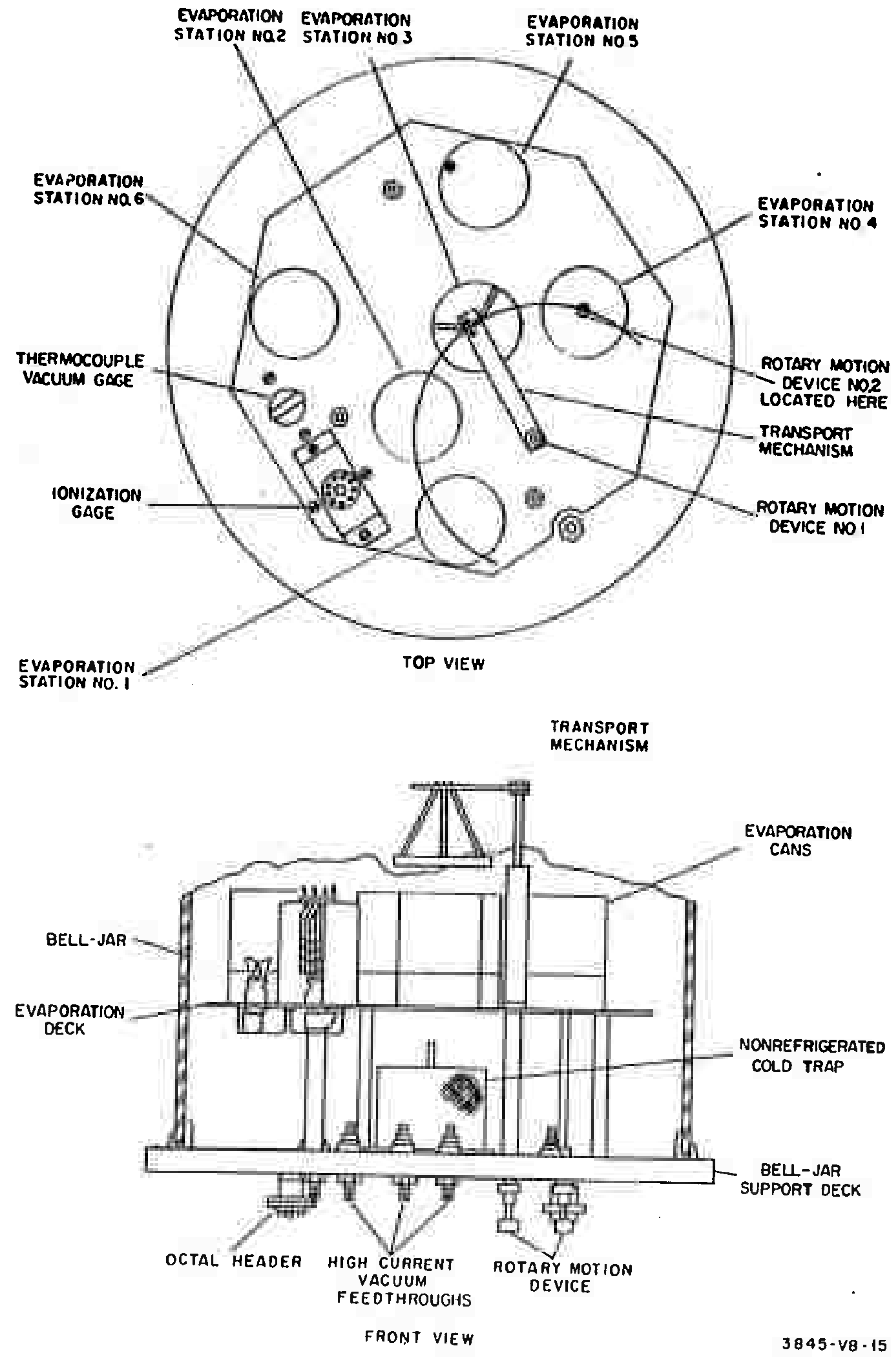

Figure 15. Sketch of Bell-Jar Processing Mechanism

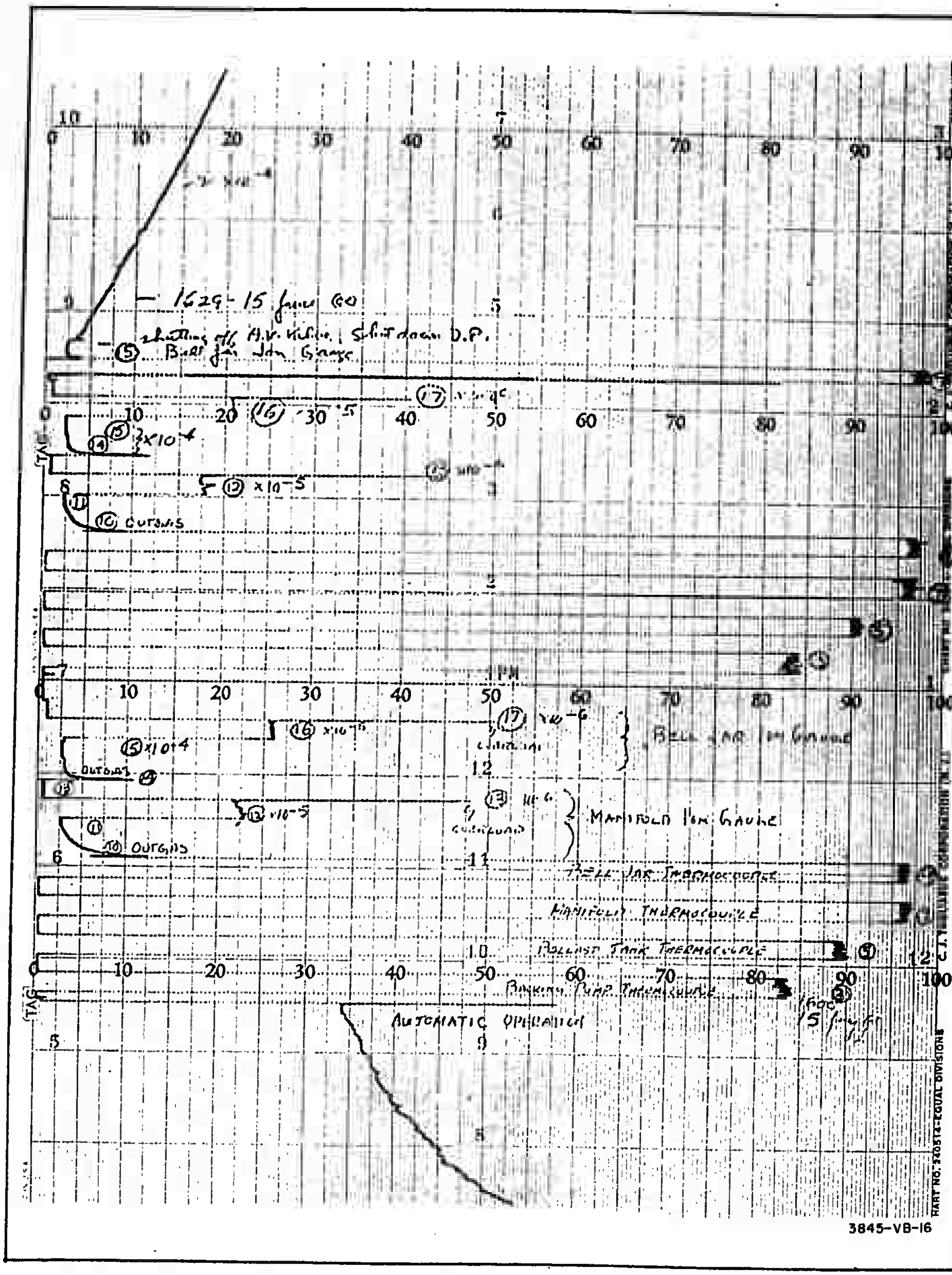

Figure 16. Strip-Chart Record Showing Automatic Readout of Vacuum Station Pressures

the ion gauge unless the pressure is below a certain value as measured by the corresponding thermocouple gauge and shutting off the ion gauge filament if the pressure reading suddenly goes off scale. Figure 17 is an example of a series of measurements made during the first bell-jar experiment. The first portion of the chart concerns measurement of the characteristics of WX-3964 No. 4, used as a comparison tube within the vacuum system during the experiment. Voltage output versus load resistance was measured for this tube, and the strip chart recorder was calibrated in terms of voltage input in the second portion of the record. The readout equipment was then put on automatic, and the third part of the record represents the pressure readings obtained throughout the vacuum system at that time.

4. 2. 3. 3 Critique

In the first semiannual report, it was stated that the guiding concepts behind the mechanical construction within the bell jar are (1) versatility, (2) capability of being cleaned readily, and capability of being exhausted to an acceptable pressure level. The system as it exists today is capable of fulfilling the first and last of these conditions, but it still lacks the capability of being cleaned readily. There have been a number of mishaps with the system, where it was necessary to disassemble and clean the contents of the bell-jar. At that time, it was found that the present construction had an excessive number of component parts, and the time and effort necessary to clean these parts was appreciable, sometimes requiring 5 days between shutdown and startup. Also, because of the large volume of the bell-jar, pumpdown to a good vacuum (1 to 5×10^{-6}) often took 2 days, a good portion of which was spent in outgassing the Biondi-Zeolite trap. Finally, however desirable, it was thought inadvisable to outgas the bell-jar by applying heat due to the possibility of implosion.

Plans are underway to supplant the bell-jar portion of the vacuum station with a glass "X" of smaller volume, as shown in figure 18. In addition to presenting a smaller pumping volume to the vacuum system, this configuration has other important advantages. It is small enough to be able to be outgassed, and the photocathode can be positioned on a wall where

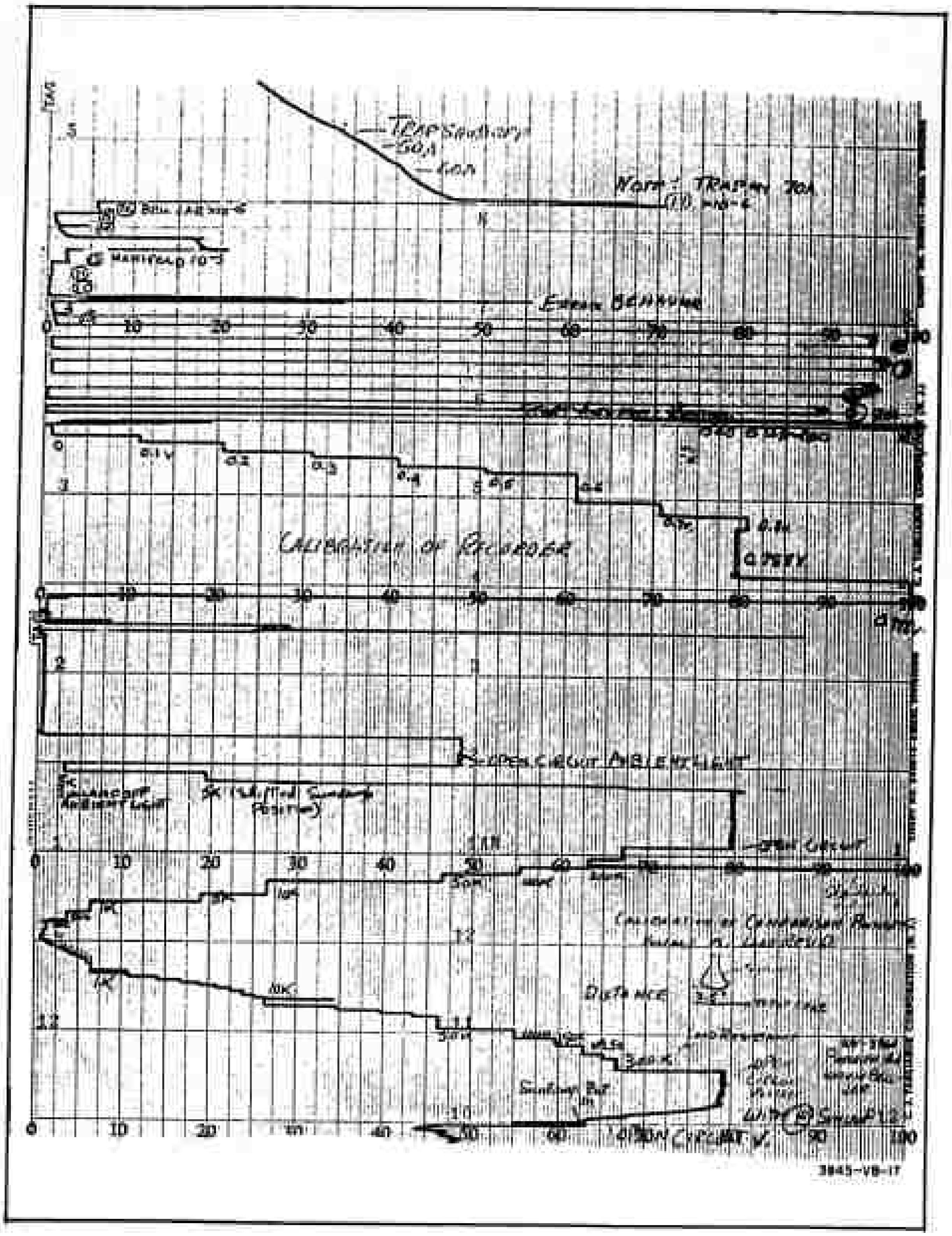

Figure 17. Strip-Chart Record Showing Electrical Measurement of Photogenerator No. 4 Characteristics

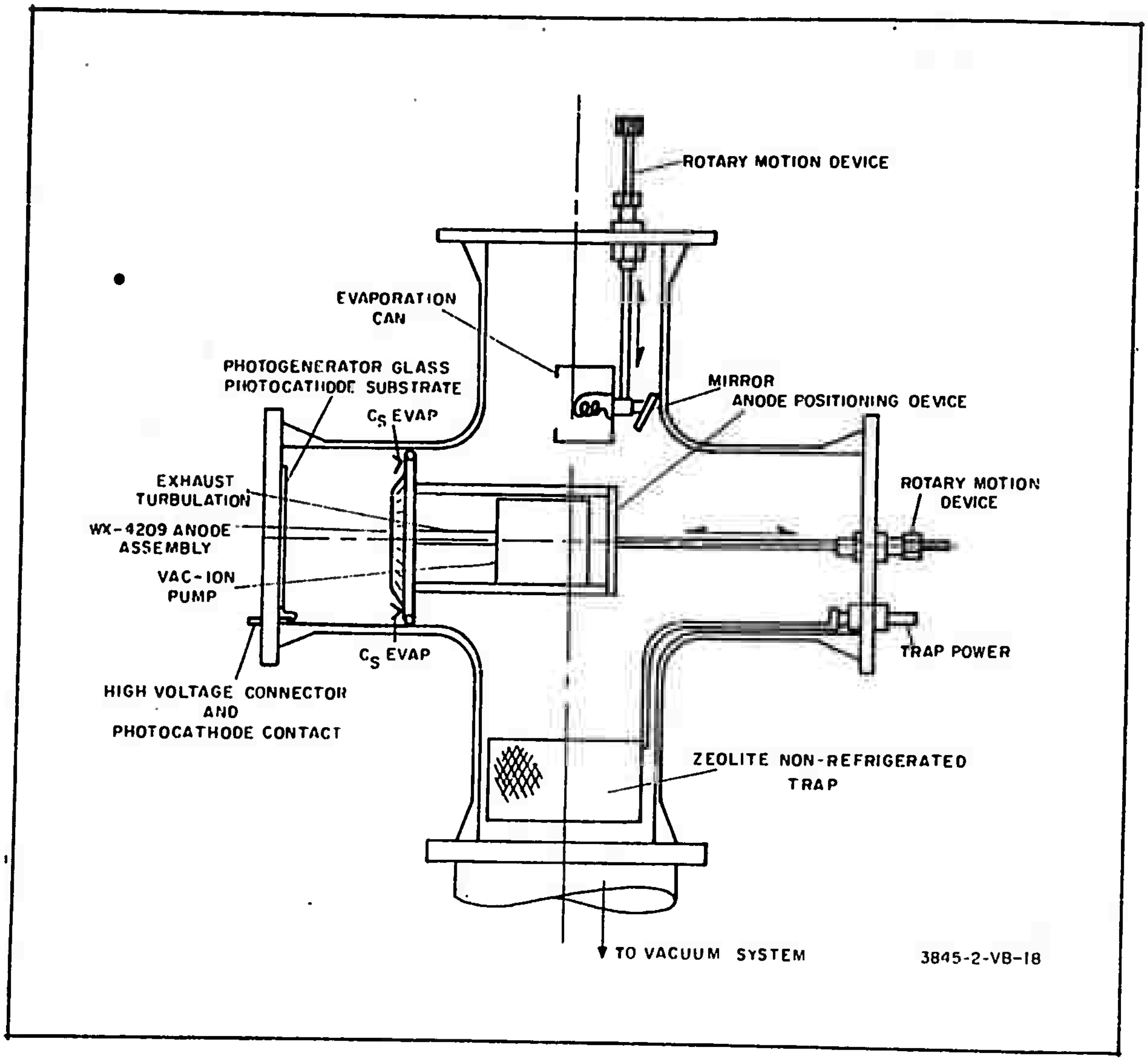

Figure 18. Sketch of Proposed Processing System

it can be heated by infrared radiation, whereas cumbersome radiative heaters must be placed within the bell-jar at present. Cesiation can take place within a much smaller volume by virtue of the movable anode positioning device which also can hold the cesium evaporators. This positioning device can also be used to make the final seal of the anode to the cathode. The evaporators may be positioned by rotary motion devices and hidden from the photocathode during outgassing. Also, the component parts would be much easier to clean, and there would be fewer parts to this system.

Although this is a most attractive alternative to the present bell-jar processing system, it is not our intention to make an immediate changeover, but a gradual building up of the proposed system with eventual replacement when all the work scheduled for the bell-jar processing station is completed. Changeover now would hinder this work and prevent the gathering of information, some of which might have a bearing upon the final design of the proposed processing system.

It should be noted that this system is adaptable to the processing of the WX-4209 as well as future photogenerators consisting of thin microsheet glass and metal mesh. Although the present design shows a vacuum-ion pump used to maintain high vacuum in the tube after it is sealed and taken out of the processing system for cesiation, the tube can also be cesiated within the small volume formed by the photocathode substrate support and the movable anode support, as shown in figure 18.

4.3 TASK B - SEALED-OFF GLASS PHOTOGENERATOR

4.3.1 Phase 1 - Bell Jar Experiment

Using the bell-jar processing system, a photocathode can be deposited upon a glass substrate and the spacing between the photocathode and anode can be varied in order to test the photogenerator concept; i.e., the elimination of the space charge limitation by decreasing the distance between photocathode and anode.

Such an experiment was attempted in April. Referring to figure 15, the antimony and manganese evaporations were performed at evaporation station No. 1, the cesium evaporation at evaporation station No. 4. A flat, stainless-steel electrode was located in place of evaporation station No. 3 for purposes of glow discharging. A WX-3964 (tube No. 4) was located at evaporation station No. 5 to act as a comparison for electrical measurements. The cesiation station consisted of a glass enclosure sealed at the bottom, the anode mesh being stretched over the top. A baffle was placed within the cesiation enclosure to prevent direct deposition of cesium upon the photocathode. This baffle was also to be used as an electrode so that (1) a field could be established between it and the anode so that the effect of repelling the electrons that had passed through the mesh could be studied, and (2) the photoemission of the anode could be measured. A Westinghouse sunlamp and a Westinghouse headlight, both powered from a constant-voltage supply, were used as light sources.

The glass substrate used for the photocathode, had a 10-mesh-per-inch copper screen etched upon it; it was placed in the transport mechanism and connected electrically to external measuring equipment. A mirror was placed underneath evaporation station No. 1 to enable light-transmission measurements to be made as described in paragraph 4. 4.

The object of this test was twofold. First, to evaporate a photosurface, and if successful, to test the photogenerator concept within the bell-jar. The second part of this test would consist of setting the spacing between the photocathode and anode, and measuring the output as a function of load resistance, while illuminated, for a series of different spacings.

The processing was as follows:

a. Bell jar pumped down to 1×10^{-6}.

b. Manganese evaporated upon photocathode substrate to give 90 percent transmission.

c. Oxygen admitted through drying filters, and the substrate glow-discharged for 30 minutes.

d. Antimony evaporated to give 65 percent transmission.

e. The photocathode substrate rotated over the cesiation can.

f. Cesium was released from 60 mg of cesium chromate-silicon powder.

After cesiation, the photocurrent measured at 40 volts positive on the anode was 0. 8 microamperes, much lower than the 17 microamperes measured with WX-3964 (No. 4) used as a comparison. With time (15 minutes), the photocurrent decreased to zero. Due to the low value of photoemission, no photogenerator action could be expected, and, indeed, no results were noted. During cesiation the photocathode substrate was at room temperature.

Analysis of the results shows several changes that must be made in the processing. Since the photoresponse dropped off while the bell-jar was being pumped, it is clear that the cesium released had not entered into the cesium antimonide reaction and was escaping. The second bell-jar experiment has provisions for heating the substrate and cesiation can up to 140°C, through the temperature range within which cesium antimonide is formed.

Also, the pumping speed of the system is high, and it is suspected that the cesium was being pumped out much too rapidly. It will be necessary to restrict the opening through which the bell-jar is being pumped by partially closing off the high vacuum valve. Finally, a greater amount of cesium (200 milligrams) will be used.

In spite of these precautions, it may not be possible to cesiate satisfactorily due to the large volume of the bell-jar and the difficulty of building up a sufficient pressure of cesium for the cesium antimonide reaction. In the next section, a parallel program is described which involves the construction of the WX-4209, a sealed glass-sandwich photogenerator.

4.3.2 Phase 2 - Sealed-Off Glass Photogenerator

In addition to being an alternate approach to the testing of the photogenerator concept, the WX-4209 has been designed to allow changes to be made in its construction as the development progresses, each of these changes testing the next step in the evolution of the thin glass photogenerator.

Figure 19 is a sketch of the WX-4209 in the first stage of development. Figure 20 is a photograph of the component parts of the tube; and figure 3 is a photograph of the anode support, with the stainless steel anode mesh welded to it, and the silicon monoxide surface applied. The anode mesh support is a drawn, machined kovar cup having sufficient rigidity to hold the mesh taut. The photocathode substrate and the glass back plates are 3/32 inch thick and can be spaced from the anode mesh support by means of thin glass rings.

The bulk of the processing of the WX-4209 will take place within the bell-jar vacuum station. The tube will be preassembled into two

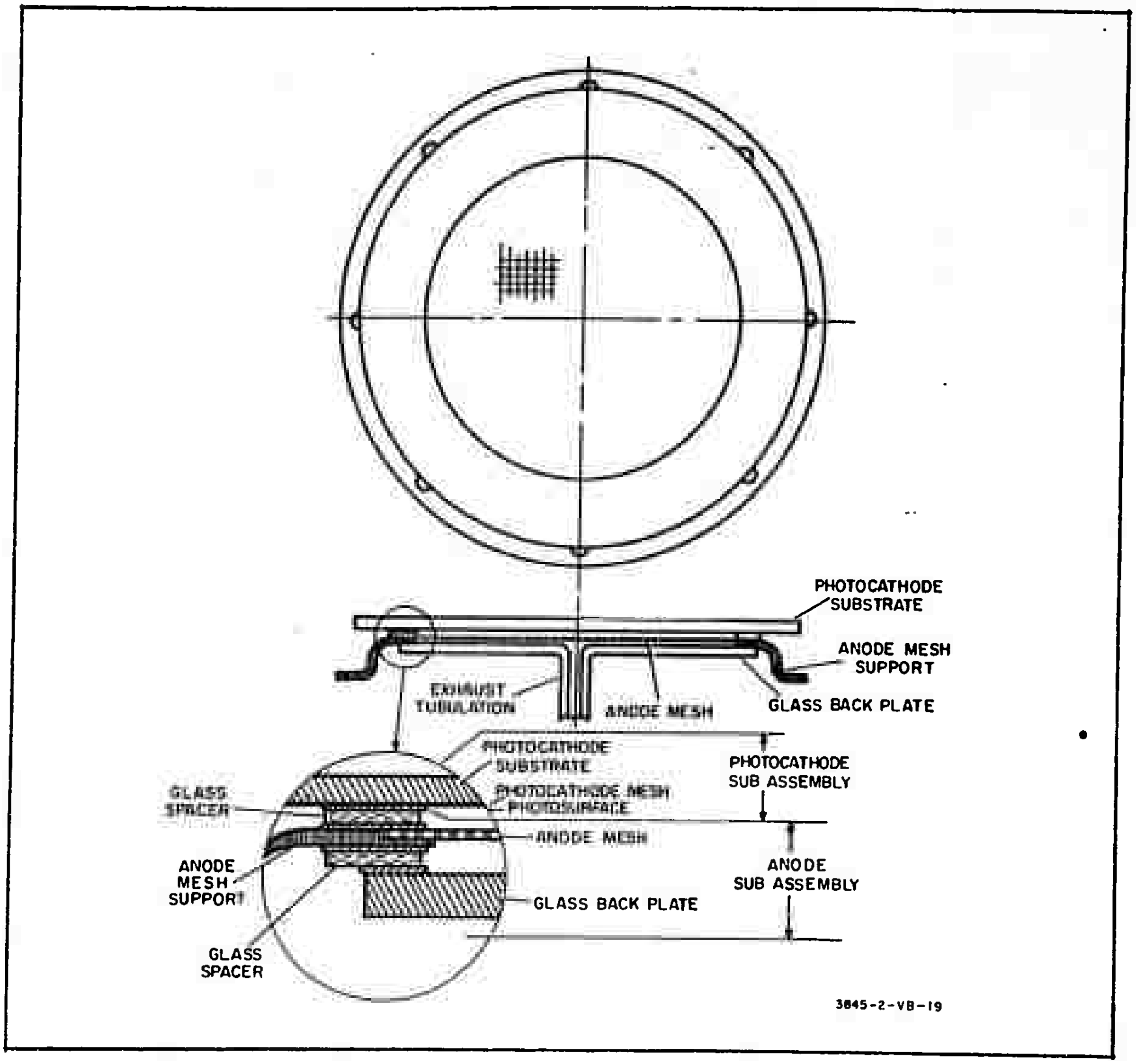

Figure 19. Sketch of Flat Glass Sandwich Photogenerator, WX-4209

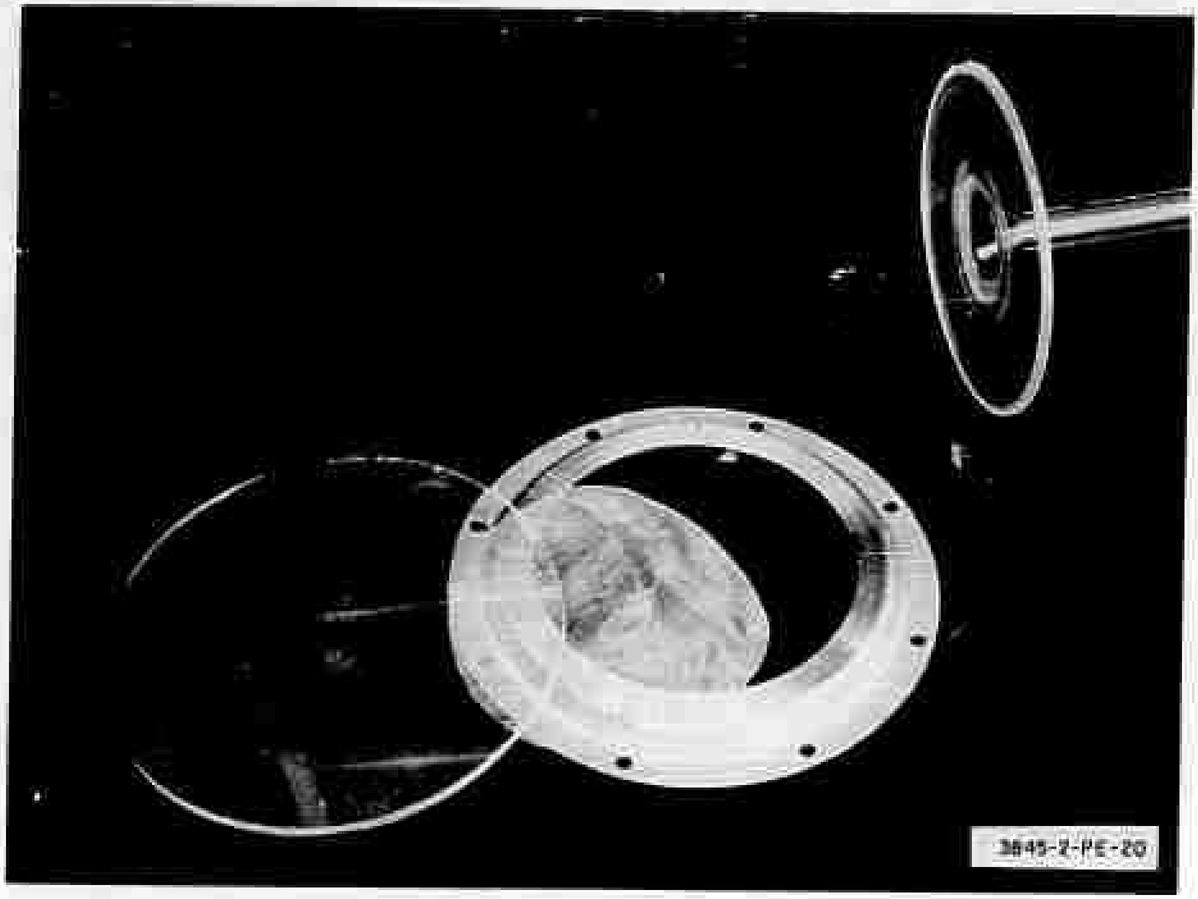

Figure 20. Component Parts of WX-4209

subassemblies, (1) the photocathode substrate, and (2) the anode assembly. The anode assembly will have a glass pumping tabulation attached to the glass backplate with a side tubulation containing cesium. The pumping tubulation will be either attached to a small 1 liter per second vac-ion pump, or sealed off in such a way that it can be opened in a vacuum. After the antimony and manganese are evaporated in the bell-jar station upon the photocathode substrate, the photocathode substrate will be assembled to the anode subassembly and the seal tested for leaks using the vac-ion pump. When the assembled photogenerator is out of the bell-jar processing system, it will then be pumped with the vac-ion pump, cesiated, and tipped off. If the tube is processed in the processing system, shown in figure 18, cesiation can be accomplished in the station, and a flat glass plate, without pumping tubulation, can be used in place of the glass backplate shown in figure 19.

Other changes can be made, for example, change the thick photocathode substrate to a thin 3 to 5 mil glass sheet, change both photocathode substrate and backplate to thin glass sheet, and finally, change the rigid anode support to a flexible anode sandwiched between two sheets of thin glass.

Present plans call for the final seal performed in the bell-jar to be made using indium, and for the anode subassembly to be joined with a high melting point solder. Figure 21 shows two glass plates sealed using a process developed by the research laboratories which calls for the solder to be applied directly to the glass and results in a vacuum tight seal. It is intended to use this process to join the component parts of the subassembly. Figure 22 is a photograph of a jig to be used for sealing the glass backplate to the metal anode mesh support.

4.4 TASK C - GLASS-PLASTIC PHOTOGENERATOR

Since this portion of the project is dependent upon the completion of Task B, little has been done. The feasibility of applying plastic to thin glass has been tested, and it was found that an epoxy ("Resiweld," H. B. Fuller, St. Paul, Minnesota) would perform this function very well. The interface was clear and the bond was resistant to shear; however, the plastic could be peeled from the glass.

It should be noted that the plastic part of the glass-plastic laminate is not being used as a vacuum envelope, but rather as a flexible strengthening support for the thin glass upon which the photocathode is deposited. The glass-plastic laminate is necessary for the added bending strength required at the earth's surface, since the photogenerator would need to withstand the handling and strain involved in its testing, assembly into a large-area power source, and storage in the space vehicle. The photogenerators would be assembled by connecting the units together by their

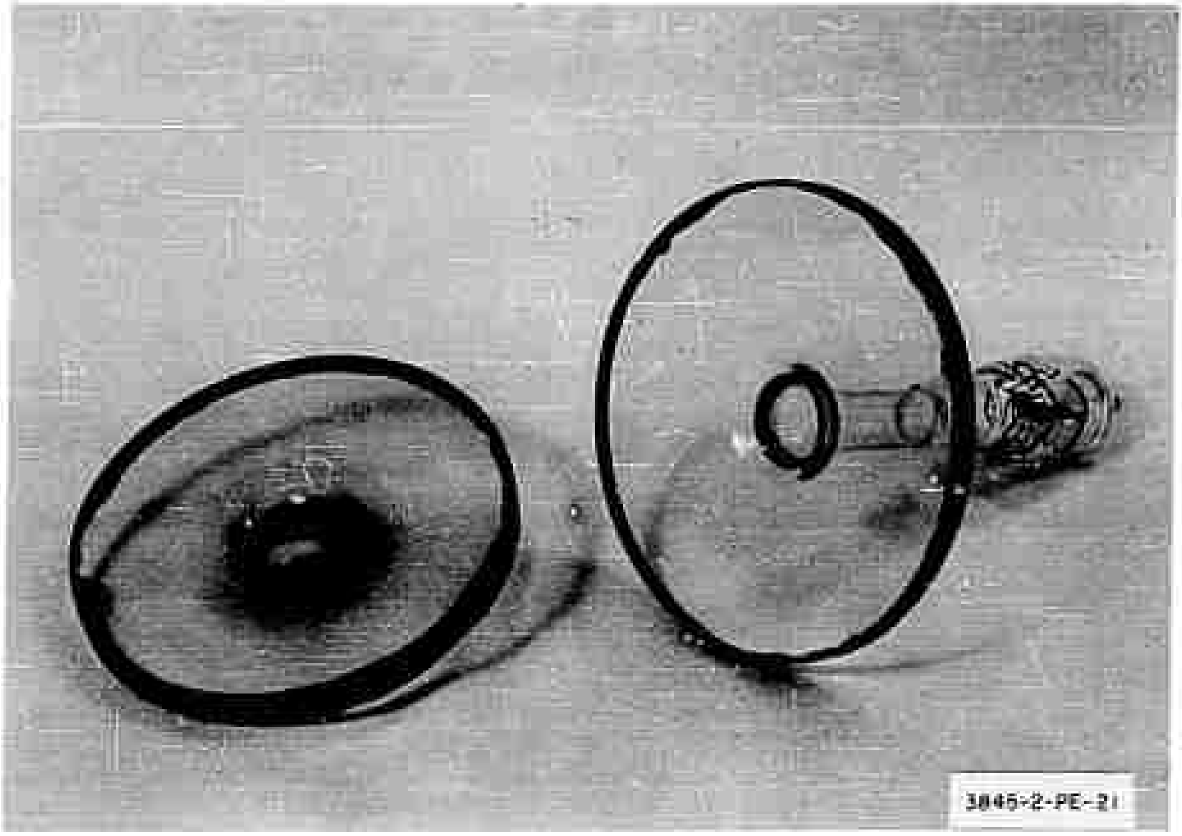

Figure 21. Test of Glass Soldering

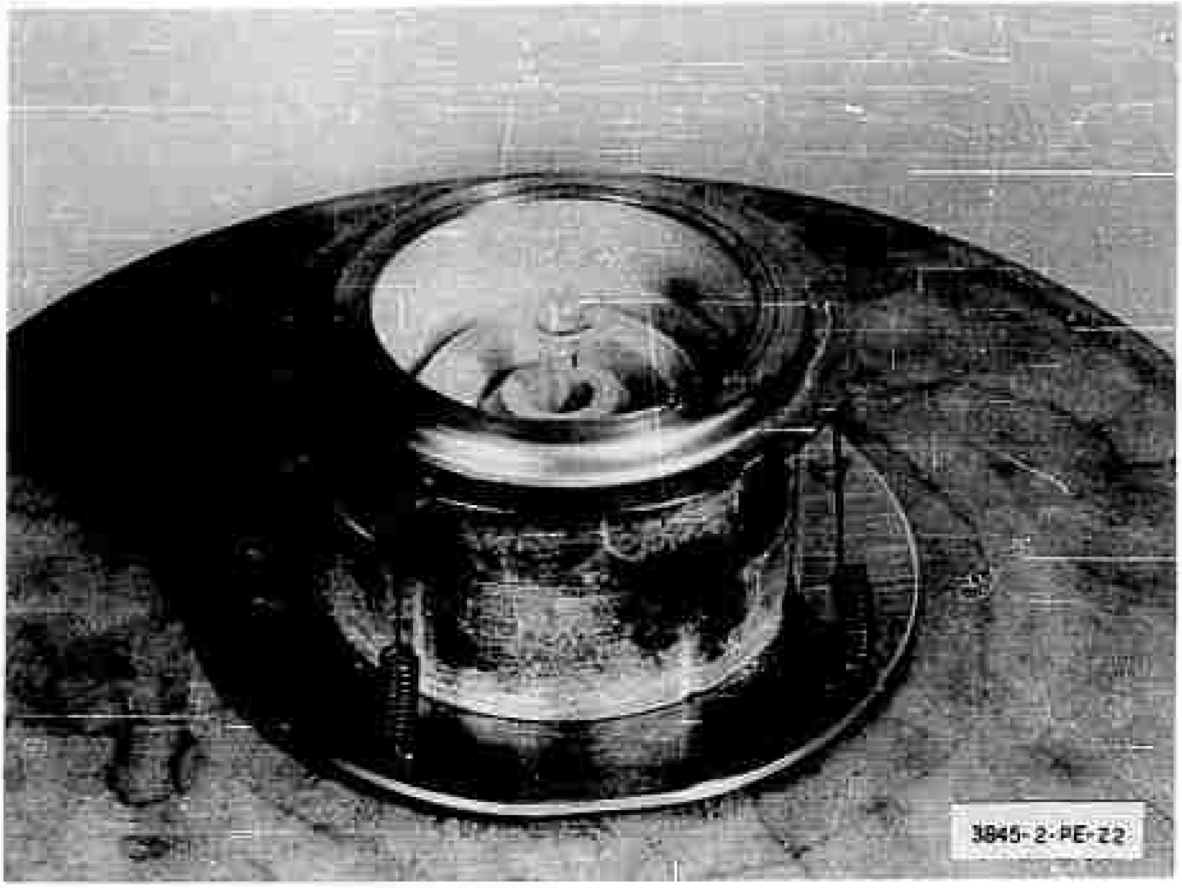

Figure 22. Soldering Jig, Anode Subassembly WX-4209

elements; i. e., anode connected physically and electrically to anode, and photocathode to photocathode. Series connections could be made by means of distribution lines which could form the semirigid support structure.

SECTION V

CONCLUSIONS

Work with the rubber-membrane potential analog has been temporarily stopped until more information is gathered from tests with the WX-3964 and from the bell-jar experiments regarding the effect of the silicon monoxide insulating coating upon the potential distribution within the tube.

The first bell-jar experiment showed that it is imperative to heat the surrounding walls and the photocathode substrate in order to form the cesium-antimonide photosurface, and that the speed of pumping should be limited to prevent pumping out the free cesium before it enters into combination with the antimony. Also, due to the large volume of the bell-jar, it is necessary to release a substantial amount of cesium; it is better to over-cesiate than to run the risk of under-cesiation.

The bell-jar processing system has operated satisfactorily and will continue to be used for the series of experiments intended to test the photogenerator concept. In the meantime, an alternate system is being designed in order to overcome certain limitations of the present system. One of the greatest limitations is the large amount of wasted volume that does not contribute to the processing. Although this could be investigated by the use of a smaller bell-jar, another limitation - that of limited accessibility to the interior - dictates another approach, a system having smaller volume and greater access to the parts being processed within. This approach, involving the use of a glass "X" as the vacuum envelope, would solve by its size another limitation - the inability of the bell-jar of the present system to be outgassed with any degree of safety. Another limitation of the present system would also lend itself quite readily to solution by the use of a glass "X"; the component parts of the present processing system must be disassembled to be cleaned, a procedure that is very wasteful of time. The component parts of a glass "X" system would be mounted on replaceable cover plates which could be made in duplicate, thereby permitting one cover plate and component parts to be in use while the other is being cleaned.

The automatic readout system has been eminently useful in conserving operating time with the vacuum station and recording experimental results for future analysis. Constant attendance at a vacuum station is not necessary, and it is possible to determine if an outgassing process is reaching completion by noting the slope of the line on the strip-chart recorder. Pertinent data relating to the course of the experiment can also be appended to the strip chart so that a complete record of a given experiment can be made with the minimum of effort.

Whereas the WX-3964 tube was not successful in determining the proper anode surface conditions necessary for efficient photogenerator action, it provided the opportunity of establishing test techniques for photogenerators, in general, and led to the useful concept of representing the photogenerator by an equivalent circuit. Several seemingly anomalous results obtained with the WX-3964 photogenerator were resolved satisfactorily; for example, some tubes exhibited a decrease in open-circuit voltage when the light source was brought closer to the tube. This could be explained by assuming that the reverse current due to photoemission from the anode had increased thereby causing the open circuit voltage to drop. This increase in reverse current could be caused by surfaces other than the photocathode emitting photoelectrons and could be approximated by another voltage generator with internal impedance connected across the output terminals (Appendix A). At present, only a qualitative comparison of the experimental data with the theoretical equivalent circuit is possible; eventually it is hoped that it will be possible to fit the experimental data better to the equivalent circuit.

The tentative design of the WX-4209 photogenerator is intended to provide the maximum flexibility in the development of this tube from the rigid, thick glass substrate photogenerator to the thin photogenerator with 3- to 5-mil glass substrate, encased in plastic. It can be processed in either the present bell-jar system or the proposed future processing system, the latter being preferred for the later stages of the development. At present, the main problem is the joining of the various pieces together in such a way that a vacuum seal is made, as well as a mechanical bond. It is expected that the final seal is to be made with indium within the processing system. If heat is applied during this seal, the tube must be cesiated after sealing, since the relatively high temperature necessary for joining the photosurface to the anode structure might cause redistribution of the cesium within the tube. Also, the anode subassembly must be joined with a higher temperature solder than that used for the final seal.

Measurement of the WX-3964 photogenerators has shown a trend of higher power output with decreasing anode-to-photocathode spacing, as predicted by the theoretical analysis. A greater amount of substantiating evidence must be obtained; however, before this trend can be firmly established, and this evidence should be collected in the series of bell-jar experiments scheduled for the next interval. In addition to establishing the relation between power output and spacing between the elements, the effect of the photosurface sensitivity and degree of vacuum can be evaluated during the bell-jar experiments. From this data, it will be possible to estimate the performance of future tubes, the WX-4209, for example.

SECTION VI

PROGRAM FOR THE NEXT INTERVAL

Work during the next interval will be directed toward the gathering of data relating the power output, the internal resistance, and the conversion efficiency of the photogenerator with respect to photocathode-anode spacing and photosurface sensitivity. Experiments will endeavor to reduce this spacing to a minimum. Also, the stability of the photosurface within the bell-jar processing station over a period of time and at different degrees of vacuum will be investigated.

The second bell-jar experiment will be completed to produce an experimental photogenerator satisfactory for these measurements. After completing the analysis of this experiment, a third experiment will be scheduled and completed. A sufficient number of photoemission control tubes WX-4220 will be made, with design changes made if necessary, to augment and direct the conduct of the bell-jar experiments.

The WX-3964 photogenerators will be completed by the Camera Tube Section and tested to obtain similar data for comparison. Three of the WX-3964 tubes will have their photosurfaces prepared and will be processed on the vacuum systems in the Baltimore Laboratory of the Special Electron Devices Section.

SECTION VII

IDENTIFICATION OF PERSONNEL

7.1 PERSONNEL ASSIGNED

IGOR LIMANSKY (2086 hrs., 28.5% of Total Effort to Date)

Education

University of Rochester, B.S. in Mechanical Engineering, 1945

New York University, M.S. in Electrical Engineering, 1953

University of Michigan, M.S. in Nuclear Engineering, 1957

Professional Experience

1947-1955 - Amperex Electronic Corporation, Hicksville, Long Island, New York. Engineer. Designed a variety of test equipment to check hydrogen thyratrons, magnetrons, high-voltage rectifiers, and geiger tubes.

1955-1959 - The Martin Company, Baltimore, Maryland. Senior Engineer. Circuit design engineering, pulse and wide-band VHF amplifier.

Since 1959 - Electronic Tube Division of Westinghouse Electric Corp., Baltimore, Maryland. Senior Engineer. Development work on special electron devices.

Military Service

1943-1946 - U.S.M.C.R. Participated in the occupation of North China.

Accomplishments

Two papers on hydrogen thyratron jitter given at the Third and Fourth Hydrogen Thyratron Symposium.

Affiliations

Member of the IRE

American Physical Society

ARTHUR S. JENSEN (546 hrs., 7.4% of Total Effort to Date)

Education

University of Pennsylvania, B.S., 1938

University of Pennsylvania, M.S. in Physics, 1939

University of Pennsylvania, Ph.D. in Physics, 1941

Professional Experience

1941 - Naval Research Laboratory, Washington, D.C. Research Physicist. Research in radar circuits.

1945-1957 - RCA Laboratories, Princeton, New Jersey. Research Physicist. Research and invention in fields of storage tubes (The Radechon), switching and coding tubes, pulse amplitude analyzers, color television systems, bandwidth compression, panel displays, gas discharges, secondary emission of insulators.

Since 1957 - Electronic Tube Division of Westinghouse Electric Corporation, Baltimore, Maryland. Section Manager. Direct research and invention in fields of storage tubes, switching and coding tubes, photoelectric devices, infrared detectors, and other special electron devices.

Military Service

1941-1945 - U.S. Navy. Officer-Instructor in Physics, U.S. Naval Academy, Department of Electrical Engineering. Captain, USNR.

Accomplishments

Eight patents have been issued, four patents are pending, and ten Westinghouse disclosures are in process.

Fifteen articles in Phys Rev., RCA Rev, Amer. J. Phys, etc.

Affiliations

Senior Member of the IRE.

Editor of "The P.S.," Local Bulletin of the Princeton Section of the IRE, 1955 and 1956.

Member of the IRE sub-committee, 7.10, Storage Tubes.

Member of American Physical Society, American Association of Physics Teachers, AAAS, U. S. Naval Research Reserve, Pi Mu Epsilon, and Sigma Xi.

MELVIN P. SIEDBAND (16 hrs., 0.5% of Total Effort to Date)

Education

University of Washington, B. A. in Mathematics, 1951

Professional Experience

1952-1956	- Air Arm Division of Westinghouse Electric Corporation, Baltimore, Maryland. Design Engineer. Work on aircraft radar systems, track-while-scan, infrared, also circuit design and magnetic amplifier development.
1956-1957	- Hoover Electronics Company, Baltimore, Maryland. Project Engineer. Work on telemetering systems, missile range timing equipment and digital computer test system.
1954-1958	- (Part time) - Melmo Scientific Company, Baltimore, Maryland. Half Owner. Manufacturing laboratory power supplies.
1957-1959	- Air Arm Division of Westinghouse Electric Corporation, Baltimore, Maryland. Project Engineer. Work on establishing a program for the automatic testing of missile radar systems. Designing automatic test equipment.
1959	- Electronic Tube Division of Westinghouse Electric Corporation, Baltimore, Maryland. Senior Engineer. Design electronic portion of equipment used in development of improved storage tubes.

Military Service

1946-1948 - U.S. Army, Radio Instructor

Accomplishments

Approximately twenty patents issued or pending, out of more than fifty patent disclosures.

Paper at NAECON, Dayton, May 5, 1959 "Logical Event and Time Period Testing as Applied to Automatic Test Equipment."

Affiliations

Member of the IRE.

EDWIN F. WOOD (1791 hrs., 24.4% of Total Effort to Date)

Education

Rochester Institute of Technology, A.A.S. in Chemistry, 1954.

Rochester Institude of Technology, B.S. in Industrial Chemistry, 1956.

Professional Experience

1951-1953 - Westinghouse Electronic Tube Division, Elmira, New York, Laboratory Technician in Applications Engineering.

1953-1955 - Navy Ordnance Division, Eastman Kodak Company, Rochester, New York. Technician in Metal Plating, Metallurgical, Analytical, Plastic, and Quality Control Laboratories.

1956-1958 - RCA Electron Tube Division, Harrison, New Jersey. Associate Engineer. Chemical and Physical Laboratory. Development work on vacuum tube materials and processing.

1958-1959 - Nicolet Industries, Florham Park, New Jersey. Chemist. Research and analytical development work on asbestos products and fiberglass-plastic laminates.

1959 - Electronic Tube Division of Westinghouse Electric Corporation, Baltimore, Maryland. Associate Engineer. Working on development of special electron devices.

Military Service

1944-1946 - U. S. Army. Heavy weapons infantry, radio school and military police.

Accomplishments

RCA Technical Report, "The Effect and Remedies of Parasitic Oscillations during the Aging and Life-testing of Tubes."

Patent disclosure related to above concerning a device for internal suppresion of parasitic oscillations.

Affiliations

Associate Member, Institute of Radio Engineers.

Student Affiliate of American Chemical Society.

Member of American Radio Relay League.

7.2 OTHER ENGINEERING ASSISTANCE (314 hrs., 9.5% of Total Effort to Date)

7.3 TECHNICIAN SUPPORT (829 hrs., 26% of Total Effort to Date)

APPENDIX A

EQUIVALENT CIRCUIT FOR PHOTOELECTRIC GENERATOR

An equivalent circuit would prove useful in future experiments if its parameters could be related to the actual mechanics of the power generation process. Then, if analysis of data of several photogenerators shows that parameter A has a marked variation, it may be stated, with some assurance, that the associated physical process has been affected by the construction of the cell if the test method is the same.

The simplest equivalent circuit of the generator would be:

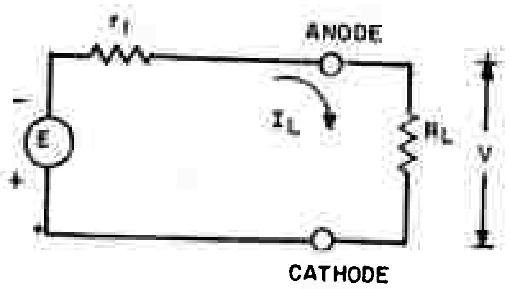

Figure 23. Simplest Equivalent Circuit

where: E is proportional to $\frac{hf}{e}$ - ϕ (work function) and is presumed constant for constant f and over operating temperature range; r_1 represents the effects of internal resistance and space charge effects and may vary with current.

This simple circuit is not very useful, however. The low work function anode will also emit electrons due to the photoelectric effect due to the photoelectric effect due to reflected light within the cell. If the equivalent circuit is to have any relation to the physical model at all, the addition of a second generator is required.

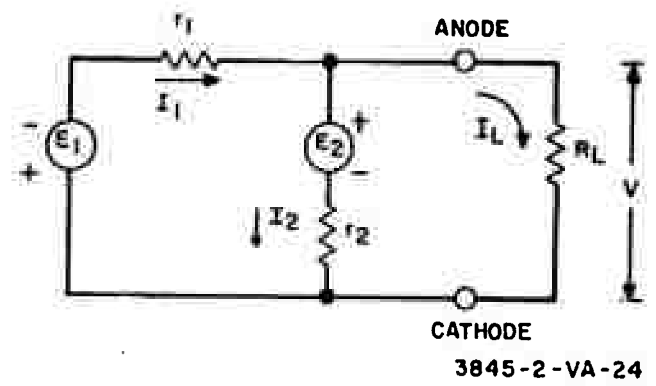

Figure 24. Equivalent Circuit With Reverse Current

In addition, the total internal resistance (r_{int}) of the cell includes some series resistance, thus we add R_s, giving:

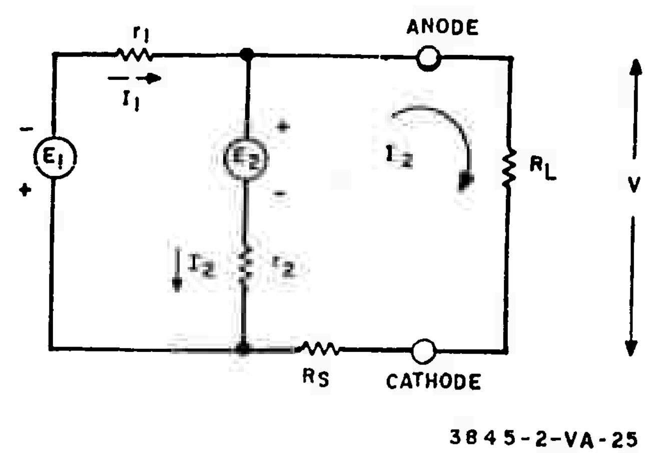

Figure 25. Equivalent Circuit With Series Resistance

This resistance will, in general, be a small component of r_{int} in a good cell.

The variation of r_1 with current is expressed most simply:

$$r_1 = A_1 I_1^{-n} \tag{A-1}$$

where: A is a function of electrode spacing, material, surface effects, etc. It will be determined from experiment.

In a space charge limited tube, we know we can write:

$$I = \frac{1}{A^{3/2}} V^{3/2} \tag{A-2}$$

an equivalent resistance expressing this can be calculated by squaring A-2

$$I^2 = \frac{1}{A^3} V^3 \tag{A-3}$$

dividing by I^3

$$I^{-1} = \frac{1}{A^3} R^3 \tag{A-4}$$

finally

$$R = A\ I^{-1/3} \tag{A-5}$$

However, we prefer to think that space charge retardation of the electrons emitted from the photocathode will not be as great as the 3/2 power law indicates. For one thing, the design aim is to reduce the space charge between the cathode and anode. For this reason, we try a square law relation

$$I \approx V^2 \tag{A-6}$$

giving

$$R = A\ I^{-1/2} \tag{A-7}$$

Then, using both approaches to get a theoretical output of V as a function of R_L, the comparison of this output with experimental values (using some simple statistical approach) will provide an answer to questions concerning space change effects. The procedure is outlined below.

For example:

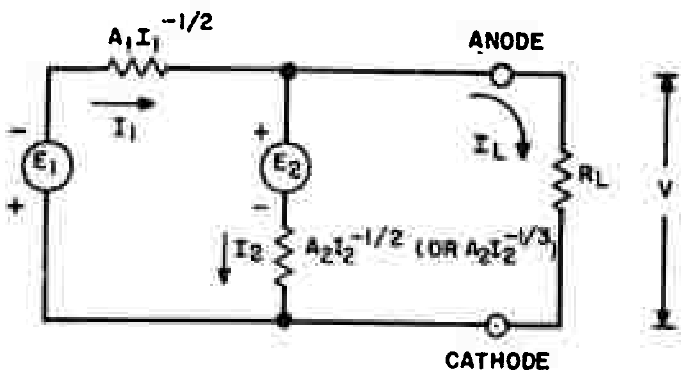

3845-2-VA-26

Figure 26. Equivalent Circuit Evaluated

V, or I_L, and R_L may be measured. We wish to evaluate A_1, A_2, E_1, and E_2.

Writing circuit equations

$$\left(A_1 I_1^{1/2}\right) = E_1 - V$$

$$I_1 = \left(\frac{E_1 - V}{A_1}\right)^2 \qquad \text{(A-8)}$$

and

$$\left(A_2 I_2^{1/2}\right) I_2 = E_2 + V$$

$$I_2 = \left(\frac{E_2 + V}{A_2}\right)^2 \qquad \text{(A-9)}$$

since

$$I_L = I_1 - I_2$$

$$I_L = \left(\frac{E_1 - V}{A_2}\right)^2 - \left(\frac{E_2 + V}{A_2}\right)^2 \qquad \text{(A-10)}$$

or

$$\frac{V}{R_L} = \left(\frac{E_1 - V}{A_1}\right)^2 - \left(\frac{E_2 + V}{A_2}\right)^2 \qquad \text{(A-11)}$$

Expanding to quadratic form

$$\left(\frac{1}{A_1^2} - \frac{1}{A_2^2}\right) V^2 - \left[\frac{1}{R_L} + 2\left(\frac{E_1}{A_1^2} - \frac{E_2}{A_2^2}\right)\right] V + \left[\frac{E_1^2}{A_1^2} - \frac{E_2^2}{A_2^2}\right] = 0 \qquad \text{(A-12)}$$

If no computer program existed, it would be simpler to write

$$f\,(V_o\ R_L) = \frac{V}{R_L} + \left(\frac{E_2 + V}{A_2}\right)^2 - \left(\frac{E_1 - V}{A_1}\right)^2 = 0 \qquad \text{(A-13)}$$

and using computer direct search methods, minimize

$$S^2 = \sum_{i=1}^{n} \left[f\,(V_i,\ R_{L_i})\right]^2 \qquad \text{(A-14)}$$

to find A_1, A_2, E_1, and E_2 directly.

Thus, not only are the constants evaluated for comparison of one photogenerator with another, but the relative values of S^2 obtained with the same photogenerator data using different equivalent circuits would enable the best equivalent circuit to be found. This, of course, will check the validity of the assumptions made as to space charge effects.

The accompanying graph (figure 27) of internal resistance of the photogenerator (r_{int}) versus load current (I_L) compares theoretical values based on an equivalent circuit, and some experimental results. The similarity is immediately obvious, only the theoretical constants must be changed to bring the computed curves into the position of the experimental one.

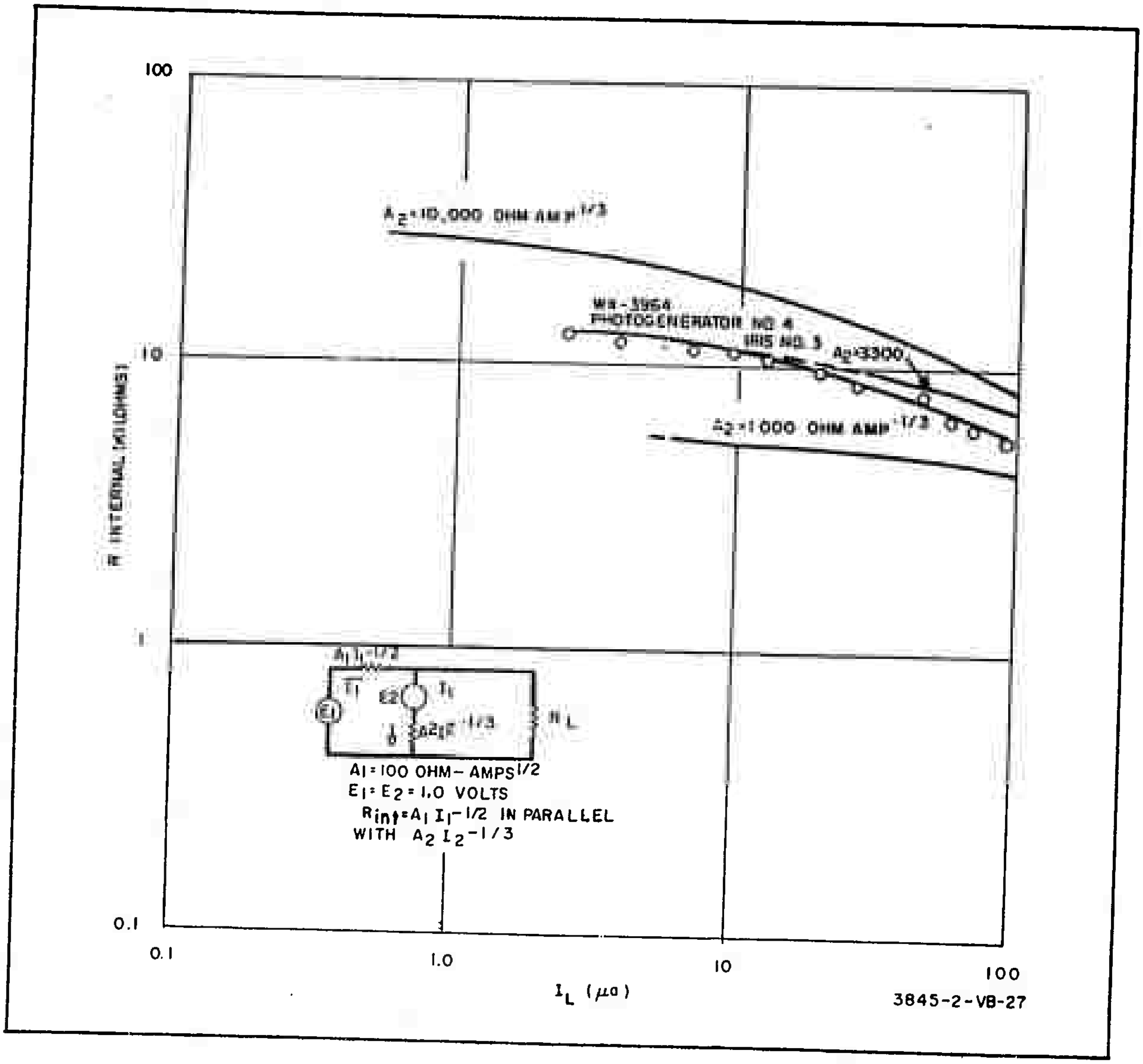

Figure 27. Graph of Internal Resistance of the Photogenerator

A number of theoretical curves were plotted in order to get a rough idea of the limits of A_1 and A_2. This will minimize computer time if direct search methods are used. This computation (refer to figure 26) was done as follows.

Since

$$E_1 = A_1 I_1^{-1/2} I_1 + V$$

$$E_1 = A_1 I_1^{1/2} + V$$

and

$$E_2 = A_2 I_2^{2/3} - V$$

Then

$$E_1 + E_2 = A_1 I_1^{1/2} + A_2 I_2^{2/3} \qquad \text{(A-15)}$$

Substituting

$$I_2 = I_1 - I_L$$

we get

$$E_1 + E_2 = A_1 I_1^{1/2} + A_2 (I_1 - I_L)^{2/3}$$

$$I_L = I_1 - \left[\frac{E_2 + \left(E_1 - A_1 I_1^{1/2}\right)}{A_2}\right]^{3/2} \qquad \text{(A-16)}$$

or

$$I_L = I_1 - \left[\frac{E_2 + V}{A_2}\right]^{3/2} \qquad \text{(A-17)}$$

since

$$V = E_1 - A_1 I_1^{1/2} \tag{A-18}$$

V may be found by assuming values of E_1, A_1, and I_1. The first two are fixed, the last varies. The range of I_1 may be found, however.

We are not interested in negative V, that is in a reversed output current. The basic design of the photogenerator precludes such a thing happening. Therefore, the maximum I_1 comes when

$$A_1 I_1^{1/2} = E_1$$

$$A_{1\,max} = \left(\frac{E_1}{A_1}\right)^2$$

also

$$I_L = I_1 - I_2$$

and $I_2 \leq I_1$ for the reason stated above. $I_{1\,min}$ must come when $I_L = 0$; that is on open circuit. Then $I_2 = I_1 = I_{oc}$. From equation A-15

$$E_1 + E_2 = A_1 I_1^{1/2} + A_2 I_2^{2/3}$$

$$\frac{E_1 + A_2}{A_2} = \frac{A_1}{A_2} I_{oc}^{1/2} + I_{oc}^{2/3}$$

$$\log \frac{E_1 + A_2}{A_2} = \log \left[\frac{A_1}{A_2} I_{oc}^{1/2} + I_{oc}^{2/3}\right] \tag{A-19}$$

This can be plotted where $\frac{E_1 + E_2}{A2}$ is ordinate and log I_{oc} is abscissa. With E_1, E_2, A_1, and A_2 chosen, I_{oc} may be found if curves have been plotted for various ratios of A_1/A_2.

In the same manner similar curves were plotted for the case where

$$r_1 = A_1 I_1^{-1/3}$$

$$r_2 = A_2 I_2^{-1/2}$$

when the exponents are equal I_{oc} may be calculated directly

$$I_{oc} = \left(\frac{E_1 + E_2}{A_1 + A_2}\right)^n \tag{A-20}$$

where, so far, n = 2 or 3.

Now values of I_1 may be tried within the interval found above and values of I_L computed using equation A-17.

From equation A-18, we know

$$V_{oc} = E_1 - A_1 I_{oc}^{1/2}$$

and the difference between this and the V computed for another value of I_1 represents the drop across the effective internal resistance. Thus

$$r_{internal} = \frac{V_{oc} - V}{I_L}$$

Moreover, power output is V I_L so that over the set range of I_1, theoretical plots of r_{int}, P_{out}, V_2 versus R_L or I_L may be made.

APPENDIX B

AUTOMATIC READOUT VACUUM MONITORING SYSTEM

This (see figure 28) consists of two chassis, power supply and amplifier-switching chassis. The power supply consists of the main d-c power supply providing regulated power for the operational amplifier and four transistor current-regulated sources for thermocouple vacuum gauges. The amplifier-switch chassis has a chopper-stabilized operational amplifier which is controlled by a stepping switch for both gain and input selection. A thyratron timing circuit controls the stepping switch so that each step may be independently timed; that is, the duration of each step may be separately determined if desired. The last step locks out the thyratron until a timing motor once again starts the sequence of 25 steps. The different positions of the stepping switch are used to control a recording chart monitor, to select the inputs to the operational amplifier such as the thermocouple gauges and ion gauges, and also to control a logic circuit preventing the vacuum gauges from becoming energized unless the thermocouple gauges show sufficient vacuum to preclude damage to the ion gauge. The ion gauge heaters are controlled as a function of grid current by means of a tube-controlled magnetic amplifier. The system contains manual bypass and stepping switch advance controls for manual operation and ease in making the initial setup. When used to operate a chart recorder, readout may be made one, two, or three times per hour, which will display complete readings of the vacuum conditions throughout the system.

The sequence of readout is as follows:

a. Delay

b. Start chart

c. Backing pump thermocouple

d. Zero reference

e. Ballast tank thermocouple

f. Zero reference

g. Manifold thermocouple

h. Zero reference

i. Bell-jar thermocouple

j. Manifold ion-gauge, Outgas and read 10^{-4}

k. Manifold ion-gauge - 10^{-4}

l. Manifold ion-gauge 10^{-5}

m. Bell-Jar ion-gauge - Outgas and Read 10^{-4}

o. Bell-Jar ion-gauge 10^{-4}

p. Bell-Jar ion-gauge 10^{-5}

q. Bell-Jar ion-gauge 10^{-6}

r. Zero reference

s. Delay

t. Thermocouple No. 1

u. Thermocouple No. 2

v. Off

w, x, y. Spare

z. One-hour delay

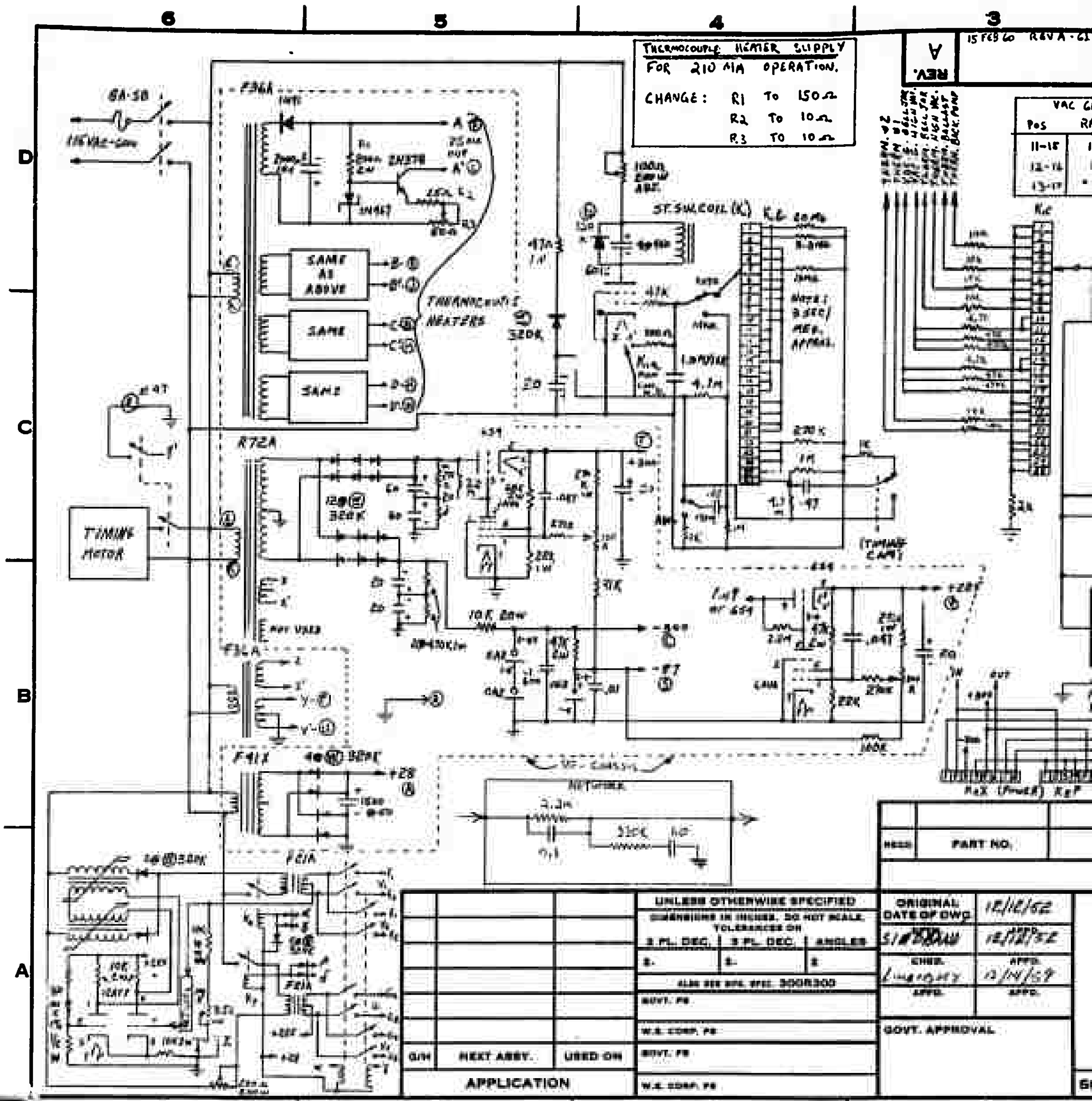
THERMOCOUPLE HEATER SUPPLY
FOR 210 MA OPERATION.
CHANGE: R1 TO 150Ω
R2 TO 10Ω
R3 TO 10Ω
REV.
A
SAME AS ABOVE
SAME
THERMOCOUPLE HEATERS
TIMING MOTOR
NETWORK
PART NO.
UNLESS OTHERWISE SPECIFIED
ORIGINAL DATE OF DWG
GOVT. APPROVAL
NEXT ASSY.
USED ON
APPLICATION

Figu

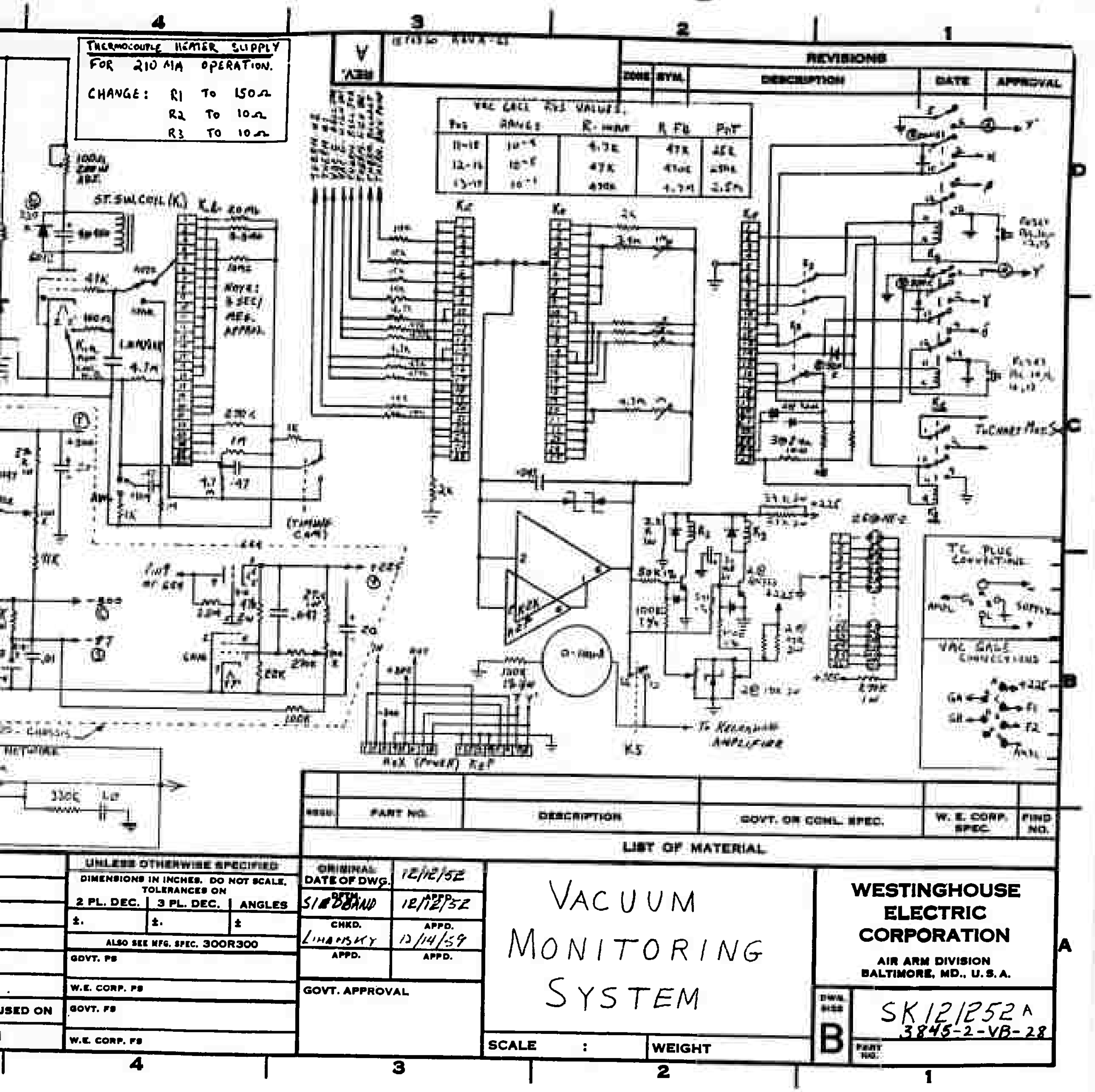

Figure 28. Vacuum Monitoring System

2

APPENDIX C

CLEANING AND HANDLING TECHNIQUES

The techniques of parts and materials preparation for the project is generally broken up into the following phases: cleaning, storage, and transfer. The common sense applications of the fundamental principles of chemistry and physics have been applied in all cases to control and supplement the existing "cook-book" recipes.

For specific cleaning schedules, refer to Section 4.2.2.3 of Report No. 3485, "The Photoemission Solar Energy Converter," by A. S. Jensen, Igor Limansky, and others, September 1959 through December 1959. The following changes are to be noted:

a. Stainless Steel

After the general cleaning schedule (step No. 2), the parts are depassivated in hot 5-percent sulfuric acid and then immersed in stainless steel bright dip.

b. Glass

All glass parts are immersed in a hot solution of 15-percent trisodium phosphate and 10-percent sodium hydroxide followed by a rinse in running tap water and immersion in 5-percent hydrofluoric acid for no more than 30 seconds. The glass parts are not stored in Kimwipes, but transferred immediately to a drying oven after rinsing in deionized water and a jet of methanol.

The general cleaning and handling schedule which applies to nearly all parts and materials is as follows:

a. Immersion in a degreaser such as trichlorethylene, or acetone, and the application of ultrasonic vibrations to remove grease and loosely adhered foreign particles.

b. Immersion in hot 5-percent acetic acid solution to remove zinc, cadmium, and other metals with high vapor pressures.

c. Immersion in a specific solvent, bright dip, etch, or detergent to place the surface in a condition with the least amount of contamination.

d. Rinse in a fast moving jet of hot tap water, followed by a rinse in a stream of deionized water.

e. Rinse in a jet of methanol, followed by a jet of acetone from polyethylene "squeeze" bottles.

f. Dry in a hot air blast, followed by storage in a dessicator over either barium oxide or activated alumina as a dessicant. Glassware and stainless steel ware are often stored in a drying oven at 120°C.

The following references of source literature have been consulted:

a. Westinghouse Process Specifications Nos. 201-7-2 through 202-3-1.

b. Biondi, et al, "Cleaning of Electronic Devices and Materials," Bell Telephone System Tech. Pub. No. 3.43; 1959

c. "Metal Finishing Guidebook," Metals and Plastics Publications, Inc. 28th Edition, 1960.

DISTRIBUTION LIST

Commanding Officer
U. S. Army Signal R&D Laboratory
Fort Monmouth, New Jersey
ATTN: SIGFM/EL-PD (1)

Dr. Norman Rosenberg
Air Force Cambridge Research Center
ATTN: CRZAP
L. G. Hanscom Field
Bedford, Massachusetts (1)

Major George W. Austin
Air Force Ballistic Missile Division
Headquarters ARDC
ATTN: WDZW
Air Force Unit Post Office
Los Angeles 45, California (1)

Mr. Rudolph A. Bradbury
Air Force Cambridge Research Center
ATTN: CRRSC
L. G. Hanscom Field
Bedford, Massachusetts (1)

Mr. Joseph B. Brauer
Rome Air Development Center
ATTN: RCSG
Griffiss Air Force Base
New York (1)

Mr. Joseph M. Hallissy, Jr.
NASA Langley Research Center
Langley Air Force Base
Virginia (1)

Mr. Milton Knight
Bureau of Aeronautics (Code AE-800)
Department of the Navy
Washington 25, D. C. (1)

Mr. George E. Thompson
Wright Air Development
ATTN: WCLEP
Wright-Patterson Air Force Base
Ohio (1)

Mr. Albert E. von Doenhoft
National Aeronautics & Space Admin.
1512 H Street, N. W.
Washington 25, D. C. (1)

Mr. Paul Youngblood
Army Ballistic Missile Agency
ATTN: ORDAB-DCEG
Redstone Arsenal, Alabama (1)

Dr. Ralph Zirkind
Bureau of Aeronautics
Department of the Navy
Washington 25, D. C. (1)

Mr. R. W. Curran
Boeing Airplane Company
Seattle, Washington (1)

International Rectifier Corp.
233 Kansas Street
El Segundo, California
ATTN: Dr. C.A. Escoffery (1)

Texas Instrument Inc.
Semi Conductor Components Div.
P. O. Box 312
Dallas, Texas
ATTN: Pat Brown (1)

California Institute of Technology
4800 Oak Grove Drive
Pasadena 3, California
ATTN: Mr. K. Ray
Jet Propulsion Lab (1)

Radio Corporation of America
RCA Laboratories
Princeton, N. J.
ATTN: P. Rappaport (1)

Lockhead Aircraft Corporation
Missiles & Space Division
3251 Hanover Road
Palo Alto, California
ATTN: Dr. W. Kapp (1)

DISTRIBUTION LIST (Continued)

Shockley Transistor Corp.
391 South San Antonio Road
Mountain View, California
ATTN: Dr. W. Shockley (1)

W. R. Grace Chemical Company
Washington Research Center
Clarksville, Maryland (1)

The Eagle-Picher Company
200 9th Avenue, N. E.
Miami, Oklahoma (1)

Armour Research Foundation
10 West 35th St.
Chicago 16, Illinois (1)

Transitron Electronic Corp.
168-182 Albion Street
Wakefield, Mass. (1)

Spectrolab, Inc.
7423 Verna Avenue
North Hollywood, California (1)

General Electric Company
Monmouth District Office
43 W. Front Street
Red Bank, New Jersey (1)

Director
Advanced Research Projects Agency
Washington 25, D. C.
THRU: OCSigO,
ATTN: SIGRD-4a-3 (6)

Chief Signal Officer
Department of the Army
Washington 25, D. C.
ATTN: SIGRD-4a-3 (8)

Naval Research Laboratory
Washington 25, D. C.
ATTN: Code 54 (1)

Commanding General
Army Ballistic Missile Agency
Redstone Arsenal, Alabama (1)

Director
Astro-Electronics Division
Communications Department,
USASRDL (1)

OASD (R&E), Rm 3E-1065
The Pentagon
Washington 25, D. C.
ATTN: Technical Library (1)

Chief Signal Officer
Department of the Army
Washington 25, D. C.
ATTN: SIGPD-8b1 (2)

Chief Signal Officer
Department of the Army
Washington 25, D. C.
ATTN: SIGRD (1)

Director, U. S. Naval Research
Lab.
Washington 25, D. C.
ATTN: Code 2027 (1)

Commanding Officer & Director
U. S. Navy Electronics Lab.
San Diego 52, California (1)

Commander
Wright Air Development Division
Wright-Patterson Air Force Base,
Ohio
ATTN: WCOSI-3 (2)
ATTN: WCLEPA (1)

Commander, Air Force Cambridge
Research Center
L. G. Hanscom Field
Bedford, Massachusetts
ATTN: CROTR (1)

Commander, Rome Air
Development Center
Air Research and Development
Command
Griffiss Air Force Base, New York
ATTN: RCSSLD (1)

DISTRIBUTION LIST (Continued)

Commanding General
U. S. Army Electronic Proving Ground
Fort Huachuca, Arizona (1)

Commander
Armed Services Technical
Information Agency
Arlington Hall Station
Arlington 12, Virginia
ATTN: TIPDR (10)

Chief, West Coast Office
U.S. Army Signal R&D Laboratory
75 South Grand Ave., Bldg. 6
Pasadena 2, California (1)

Commanding Officer
U.S. Army Signal Equipment Support
Agency
Fort Monmouth, New Jersey
ATTN: SIGFM/ADJ (1)

Commanding Officer
U.S. Army Signal R&D Laboratory
Fort Monmouth, New Jersey
ATTN: SIGRA/SL-P (1)
ATTN: SIGRA/SL-PS (6)
ATTN: SIGRA/SL-ADJ (1)
ATTN: Director of Research (1)
ATTN: Tech Documents Center (1)
ATTN: SIGRA/SL-PRG (1)

Chief, U. S. Army Security Agency
Arlington Hall Station
Arlington 12, Virginia (2)

Deputy President
U.S. Army Security Agency Board
Arlington Hall Station
Arlington 12, Virginia (1)

Mr. George B. Ferguson
U.S. Army Ordnance Missile Command
ATTN: ORDXM-RR
Redstone Arsenal, Alabama (1)

Dr. Bernard Stein
Army Research Office
Office, Chief of Research &
Development
Arlington Hall Station
Arlington 12, Virginia (1)

Mr. B. James Wilson
Naval Research Laboratory
(Code 5230)
Department of the Navy
Washington 25, D.C. (1)

Mr. Frederick A. Zihlman
Bureau of Ordnance (Code RES-6B)
Department of the Navy
Main Navy Building
Washington 25, D. C. (1)

Comdr George L. Bliss
Bureau of Aeronautics (Code AE-8)
Department of the Navy
Washington 25, D. C. (1)

Major William G. Alexander
Hq. Air Research & Development
Command
ATTN: RDRAPP
Andrews Air Force Base
Washington 25, D. C. (1)

Mr. George W. Sherman
Wright Air Development Division
ATTN: WCLEE
Wright-Patterson Air Force Base
Ohio (1)

Mr. William D. Downs
Headquarters USAF
ATTN: AFDRD-AN
Washington 25, D. C. (1)

DISTRIBUTION LIST (Continued)

Mr. G. B. Wareham
Equipment & Supplies Division
Office, Fuels, Materials & Ordnance
Office, Director of Defense Research
and Engineering
Department of Defense
Washington 25, D.C. (1)

Mr. David Novik
National Aeronautics & Space Admin.
1512 H Street, N. W.
Washington 25, D. C. (1)

AD–   Div.

Westinghouse Electric Corp., Baltimore, Md.
ON THE PHOTOEMISSION SOLAR ENERGY CONVERTER
by A. S. Jensen, I. Limansky, and others. Rept. for Sep 59 through Dec 59. 48 pp. incl. illus.
(Scientific Rept. No. 1)
(Contract DA-36-039-SC 85240)   Unclassified Report

The use of photoemission as a method of converting solar photon flux into electrical power and the development of a high power-per-unit weight unit suitable for space use are considered in this study. Experimental results using the WX-3964 photogenerator are presented, showing that one tube, having a relatively wide spacing of 70 mils, supplied

(over)

UNCLASSIFIED

1. Preliminary Studies
2. Sealed-Off Glass Photogenerator
3. Rubber-Membrane Potential Analog
I. Title: Photomission Solar Energy Converter
II. Jensen, A. S.; and Limansky, I.; and others
III. U. S. Army Signal Research and Development Laboratory Fort Monmouth, N. J.

Armed Services Technical Information Agency

UNCLASSIFIED

AD–   Div.

Westinghouse Electric Corp., Baltimore, Md.
ON THE PHOTOEMISSION SOLAR ENERGY CONVERTER
by A. S. Jensen, I. Limansky, and others. Rept. for Sep 59 through Dec 59. 48 pp. incl. illus.
(Scientific Rept. No. 1)
(Contract DA-36-039-SC 85240)   Unclassified Report

The use of photoemission as a method of converting solar photon flux into electrical power and the development of a high power-per-unit weight unit suitable for space use are considered in this study. Experimental results using the WX-3964 photogenerator are presented, showing that one tube, having a relatively wide spacing of 70 mils, supplied

(over)

UNCLASSIFIED

1. Preliminary Studies
2. Sealed-Off Glass Photogenerator
3. Rubber-Membrane Potential Analog
I. Title: Photomission Solar Energy Converter
II. Jensen, A. S.; and Limansky, I.; and others
III. U. S. Army Signal Research and Development Laboratory Fort Monmouth, N. J.

Armed Services Technical Information Agency

UNCLASSIFIED

AD–   Div.

Westinghouse Electric Corp., Baltimore, Md.
ON THE PHOTOEMISSION SOLAR ENERGY CONVERTER
by A. S. Jensen, I. Limansky, and others. Rept. for Sep 59 through Dec 59. 48 pp. incl. illus.
(Scientific Rept. No. 1)
(Contract DA-36-039-SC 85240)   Unclassified Report

The use of photoemission as a method of converting solar photon flux into electrical power and the development of a high power-per-unit weight unit suitable for space use are considered in this study. Experimental results using the WX-3964 photogenerator are presented, showing that one tube, having a relatively wide spacing of 70 mils, supplied

(over)

UNCLASSIFIED

1. Preliminary Studies
2. Sealed-Off Glass Photogenerator
3. Rubber-Membrane Potential Analog
I. Title: Photomission Solar Energy Converter
II. Jensen, A. S.; and Limansky, I.; and others
III. U. S. Army Signal Research and Development Laboratory Fort Monmouth, N. J.

Armed Services Technical Information Agency

UNCLASSIFIED

AD–   Div.

Westinghouse Electric Corp., Baltimore, Md.
ON THE PHOTOEMISSION SOLAR ENERGY CONVERTER
by A. S. Jensen, I. Limansky, and others. Rept. for Sep 59 through Dec 59. 48 pp. incl. illus.
(Scientific Rept. No. 1)
(Contract DA-36-039-SC 85240)   Unclassified Report

The use of photoemission as a method of converting solar photon flux into electrical power and the development of a high power-per-unit weight unit suitable for space use are considered in this study. Experimental results using the WX-3964 photogenerator are presented, showing that one tube, having a relatively wide spacing of 70 mils, supplied

(over)

UNCLASSIFIED

1. Preliminary Studies
2. Sealed-Off Glass Photogenerator
3. Rubber-Membrane Potential Analog
I. Title: Photomission Solar Energy Converter
II. Jensen, A. S.; and Limansky, I.; and others
III. U. S. Army Signal Research and Development Laboratory Fort Monmouth, N. J.

Armed Services Technical Information Agency

UNCLASSIFIED

AD–

output power of over 125 microwatts at an efficiency of 0.01 percent. A description of an experiment in the bell-jar processing station is presented herein, and the operation of the automatic readout experiment is described. Steps leading to the manufacture and processing of the anode and photocathode are described, as well as the construction of the WX–4209, a thin glass-sandwich photogenerator. Changes in processes and procedures are noted, and work leading to an equivalent circuit for the photogenerator is given.

UNCLASSIFIED

UNITERMS

Photoemission
Power
Solar
Converter

UNCLASSIFIED

AD–

output power of over 125 microwatts at an efficiency of 0.01 percent. A description of an experiment in the bell-jar processing station is presented herein, and the operation of the automatic readout experiment is described. Steps leading to the manufacture and processing of the anode and photocathode are described, as well as the construction of the WX–4209, a thin glass-sandwich photogenerator. Changes in processes and procedures are noted, and work leading to an equivalent circuit for the photogenerator is given.

UNCLASSIFIED

UNITERMS

Photoemission
Power
Solar
Converter

UNCLASSIFIED

AD–

output power of over 125 microwatts at an efficiency of 0.01 percent. A description of an experiment io the bell-jar processiog station is preseoted herein, and the operation of the automatic readout experiment is described. Stepa leadiog to the manufacture and processing of the aoode and photocathode are described, as well as the coostruction of the WX–4209, a thin glass-sandwich photogenerator. Changea in proceases and procedures are ooted, and work leading to ao equivalent circuit for the photogenerator is given.

UNCLASSIFIED

UNITERMS

Photoemissioo
Power
Solar
Cooverter

UNCLASSIFIED

AD–

output power of over 125 microwatts at an efficiency of 0.01 percent. A description of an experiment in the bell-jar processing station is presented herein, and the operation of the automatic readout experiment is described. Steps leading to the manufacture and processing of the anode and photocathode are described, as well as the construction of the WX–4209, a thin glass-sandwich photogenerator. Changes in processes and procedures are noted, and work leading to an equivalent circuit for the photogenerator is given.

UNCLASSIFIED

UNITERMS

Photoemission
Power
Solar
Converter

UNCLASSIFIED

AD–   Div.

Westinghouse Electric Corp., Baltimore, Md.
ON THE PHOTOEMISSION SOLAR ENERGY CONVERTER
by A. S. Jensen, I. Limansky, and others. Rept. for Sep 59 through Dec 59. 48 pp. incl. illus.
(Scientific Rept. No.)
(Contract DA–36–039–SC 85248)   Unclassified Report

The use of photoemission as a method of converting solar photon flux into electrical power and the development of a high power-per-unit weight unit suitable for space use are considered in this study. Experimental results using the WX–3964 photogenerator are presented, showing that one tube, having a relatively wide spacing of 70 mils, supplied

(over)

UNCLASSIFIED

1. Preliminary Studies
2. Sealed–Off Glass Photogenerator
3. Rubber–Membrane Potential Analog
I. Title: Photomission Solar Energy Converter
II. Jensen, A. S.; and Limansky, I.; and others
III. U. S. Army Signal Research and Development Laboratory Fort Monmouth, N. J.

Armed Services Technical Information Agency

UNCLASSIFIED

AD–   Div.

Westinghouse Electric Corp., Baltimore, Md.
ON THE PHOTOEMISSION SOLAR ENERGY CONVERTER
by A. S. Jensen, I. Limansky, and others. Rept. for Sep 59 through Dec 59. 48 pp. incl. illus.
(Scientific Rept. No.)
(Contract DA–36–039–SC 85248)   Unclassified Report

The use of photoemission as a method of converting solar photon flux into electrical power and the development of a high power-per-unit weight unit suitable for space use are considered in this study. Experimental results using the WX–3964 photogenerator are presented, showing that one tube, having a relatively wide spacing of 70 mils, supplied

(over)

UNCLASSIFIED

1. Preliminary Studies
2. Sealed–Off Glass Photogenerator
3. Rubber–Membrane Potential Analog
I. Title: Photomission Solar Energy Converter
II. Jensen, A. S.; and Limansky, I.; and others
III. U. S. Army Signal Research and Development Laboratory Fort Monmouth, N. J.

Armed Services Technical Information Agency

UNCLASSIFIED

AD–   Div.

Westinghouse Electric Corp., Baltimore, Md.
ON THE PHOTOEMISSION SOLAR ENERGY CONVERTER
by A. S. Jensen, I. Limsnsky, and others. Rept. for Sep 59 through Dec 59. 48 pp. incl. illus.
(Scientific Rept. No.)
(Contract DA–36–039–SC 85248)   Unclassified Report

The use of photoemission as a method of converting solar photon flux into electrical power and the development of a high power-per-unit weight unit suitable for space use are considered in this study. Experimental results using the WX–3964 photogenerator are presented, showing that one tube, having a relatively wide spacing of 70 mils, supplied

(over)

UNCLASSIFIED

1. Preliminary Studies
2. Sealed–Off Glass Photogenerator
3. Rubber–Membrane Potential Analog
I. Title: Photomission Solar Energy Converter
II. Jensen, A. S.; and Limsnsky, I.; and others
III. U. S. Army Signal Research and Development Laboratory Fort Monmouth, N. J.

Armed Services Technical Information Agency

UNCLASSIFIED

AD–   Div.

Westinghouse Electric Corp., Baltimore, Md.
ON THE PHOTOEMISSION SOLAR ENERGY CONVERTER
by A. S. Jensen, I. Limansky, and others. Rept. for Sep 59 through Dec 59. 48 pp. incl. illus.
(Scientific Rept. No.)
(Contract DA–36–039–SC 85248)   Unclassified Report

The use of photoemission as a method of converting solar photon flux into electrical power and the development of a high power-per-unit weight unit suitable for space use are considered in this study. Experimental results using the WX–3964 photogenerator are presented, showing that one tube, having a relatively wide spacing of 70 mils, supplied

(over)

UNCLASSIFIED

1. Preliminary Studies
2. Sealed–Off Glass Photogenerator
3. Rubber–Membrane Potential Analog
I. Title: Photomission Solar Energy Converter
II. Jensen, A. S.; and Limansky, I.; and others
III. U. S. Army Signal Research and Development Laboratory Fort Monmouth, N. J.

Armed Services Technical Information Agency

UNCLASSIFIED

AD–

output power of over 125 microwatts at an efficiency of 0.01 percent. A description of an experiment in the bell-jar processing station is presented herein, and the operation of the automatic readout experiment is described. Steps leading to the manufacture and processing of the anode and photocathode are described, as well as the construction of the WX–4209, a thin glass-sandwich photogenerator. Changes in processes and procedures are noted, and work leading to an equivalent circuit for the photogenerator is given.

UNCLASSIFIED

UNITERMS

Photoemission
Power
Solar
Converter

UNCLASSIFIED

AD–

output power of over 125 microwatts at an efficiency of 0.01 percent. A description of an experiment in the bell-jar processing station is presented herein, and the operation of the automatic readout experiment is described. Steps leading to the manufacture and processing of the anode and photocathode are described, as well as the construction of the WX–4209, a thin glass-sandwich photogenerator. Changes in processes and procedures are noted, and work leading to an equivalent circuit for the photogenerator is given.

UNCLASSIFIED

UNITERMS

Photoemission
Power
Solar
Converter

UNCLASSIFIED

AD–

output power of over 125 microwatts at an efficiency of 0.01 percent. A description of an experiment in the bell-jar processing station is presented herein, and the operation of the automatic readout experiment is described. Steps leading to the manufacture and processing of the anode and photocathode are described, as well as the construction of the WX–4209, a thin glass-sandwich photogenerator. Changes in processes and procedures are noted, and work leading to an equivalent circuit for the photogenerator is given.

UNCLASSIFIED

UNITERMS

Photoemission
Power
Solar
Converter

UNCLASSIFIED

AD–

output power of over 125 microwatts at an efficiency of 0.01 percent. A description of an experiment in the bell-jar processing station is presented herein, and the operation of the automatic readout experiment is described. Steps leading to the manufacture and processing of the anode and photocathode are described, as well as the construction of the WX–4209, a thin glass-sandwich photogenerator. Changes in processes and procedures are noted, and work leading to an equivalent circuit for the photogenerator is given.

UNCLASSIFIED

UNITERMS

Photoemission
Power
Solar
Converter

UNCLASSIFIED